THE PENNSYLVANIA STATE UNIVERSITY
SCHREYER HONORS COLLEGE

DEPARTMENT OF CHEMICAL ENGINEERING

SELF-HEALING PROPERTIES OF SODA-LIME SILICATE GLASS UNDER THERMAL TREATMENT

TRAN HA-QUYNH NGO
FALL 2019

A thesis
submitted in partial fulfillment
of the requirements
for a baccalaureate degree in Chemical Engineering
with honors in Chemical Engineering

Reviewed and approved* by the following:

Seong Kim
Professor of Chemical Engineering
Professor of Materials Science and Engineering
Thesis Supervisor

Michael Janik
Professor of Chemical Engineering
Honors Adviser

* Signatures are on file in the Schreyer Honors College.

ABSTRACT

Glass self-healing properties are of high interest in the materials science world. Success in self-healing designs would play an instrumental role in material safety, fatigue lifetime, and product performance. Many industrial applications, such as fuel cells and solid oxide electrolyzers, have been hindered by the lack of long-term durability and minimized glass healing understanding. Hence, the goal of this thesis is to explore the effects of thermal treatment temperatures, annealing conditions, and water pre-treatment on the self-healing ability of soda-lime silicate glass for a further comprehension on the different factors that drive the efficiency of thermal healing.

The proposed thermal healing mechanism in glass is governed by critical morphological changes driven by viscous flow and capillary forces. The effects of thermal treatment temperature on glass healing could be understood via the inverse relationship between viscosity and temperature based on Fulcher's equation, where soda-lime silicate glass thermally treated at lower glass transition temperature performed better in crack closure. Additionally, higher annealed temperature glass carried out better healing performance compared to lower annealed temperature glass. Water pre-treatment significantly enhanced necessary morphological alterations for thermal healing due to water-glass interaction and the reduced viscosity effects. Crack propagation and pinch-off healing mechanism were observed during the thermal treatment process.

TABLE OF CONTENTS

LIST OF FIGURES

LIST OF TABLES

ACKNOWLEDGEMENTS

I would like to honor my final thesis piece to my thesis supervisor, Dr. Seong Kim, as he assisted me tremendously throughout my three years of research experience, guided me through my thesis formulation and composition process, and inspired me profoundly with his passion for understanding the intricacy of science.

I would like to thank you Dr. John Mauro for his rich experience and brilliant understanding in the field of glass science. The knowledge provided from his MATSE 415 course lays the fundamental ground for my honors thesis and for my curiosity in further exploring the immense possibilities of glass.

I would also like to thank you Hongshen Liu, Dr. Jiawei Luo, Matthew Rabii, Conghang Qu, and Ian Wietecha-Rieman for their paramount collaboration and insightful discussions. They showed me the importance of mentorship and teamwork in the tackling the great challenges in the science and engineering field.

I would also like to thank you my honors adviser, Dr. Michael Janik, for his wisdom and counseling throughout my college career. Dr. Janik is undoubtedly one of the most caring and inspirational professors I have met at Penn State. He introduced me to different research and career opportunities on campus and advised me greatly in my Chemical Engineering career path.

Finally, I would like to thank you my family and friends for their unconditional support in all my four years of college. Without them, I would not be the person I am today.

Chapter 1

Introduction

The Science of Glass

Science of the modern-day world owes its success to the invention of glass. Although the presence of glass is traced back to thousands of years ago, recent innovations of glass make them instrumental agents of the advanced materials science era. Its versatility in chemical composition and physical properties allow for diverse applications that entwined at every corner of human life.

While the definition of glass differs greatly from one spectrum to another, it is typically identified as an inorganic material that exhibits non-crystalline and nonequilibrium state of matter, appearing solid on a short time scale but continuously relaxes towards the liquid state (Varshneya, 2019). Glass is formed upon quenching of a liquid, where the crystallization phase is suspended due to sufficiently high cooling rate, thus vitrified liquid transforms into its glassy state before nucleation and crystal growth could take place (Varshneya, 2019). This results in an exclusive material that exhibits higher viscosity than a typical solid (McMillan, 1979), elastic behaviors resembling the supercooled liquid phase (Paul, 1990), and excellent insulating properties due to low numbers of free monovalent ions (Hasanuzzaman, 2015).

There is an infinite possibility for glass chemical composition, each with unique characteristics. Vitreous silica is used for mercury vapor lamps, astronomical mirrors, optical fibers, insulating layers in integrated circuits, and gas or electrical heated devices because of its high refractory, excellent chemical resistance, and outstanding ultraviolet transparency

(Sempolinski, 2000). Soda-lime silicate glass is commonly found in many commercialized applications such as windowpanes, glass containers for beverages, and fluorescent lamp envelopes due to its low cost and good chemical durability (Varshneya, 2019). Borosilicate glass, with its low thermal expansion coefficient and exceptional resistance to chemical attack (Varshneya, 2019), is used for implantable medical devices (Wananuruksawong, 2011), microwave- and dishwasher-safe cookware (Estes, 2019), commercial broadcast transmitters, and laboratory glassware. Lead silicate glass is applicable in radiation shielding for its X-ray absorption behaviors (Hasanuzzaman, 2015) and decorative household glassware for its large working range (Benvenuto, 2015). Aluminosilicate glass plays a crucial role in flat-panel displays (with the introduction of Corning Gorilla Glass® for smartphone screens), fiberglass insulation, thermometers, and combustion tubes (Hasanuzzaman, 2015). Boron oxide- and phosphate oxide-based glass make great candidates in the biomedical industry for bone tissue repair and regeneration (Mancuso, 2017). Vanadium dioxide-based glass provides smart coatings for commercial applications, construction industry, and transportation sectors due to its environmental stability over a long-time period, high phase transition temperature, and optical properties (Chang, 2018 and Berger, 2012). Chalcogenide glass is used for important optoelectronic applications, including infrared detectors and infrared optical fibers, due to its non-linear optical effects and electron-induced permittivity modification (Sagadevan, 2014). Overall, glass embraces endless potentials, weaving in every facet of human life.

Although the existence of glass traces back to several thousand years ago, glass remained an unnoticed subject for a long period of time. It was not until very recently that the field of glass science was given a formal platform to thrive. In the past century, tremendous research has been dedicated to the understanding of glass – its glassy state structural basis, the glass transition and

relaxation phenomenon, and molecular modelling. Hence, the fundamental comprehension of glass allows scientists and engineers to carry out innovations to meet the ever-changing societal needs. Glass has been modified to become stronger, versatile, flexible, and durable. From a material that was only used to contain, glass now moves information at speed of light, enables devices that are sophisticated, transforms everyday surfaces, and provides extraordinary benefits (Corning). In the Glass Age today, glass science continues to exert its importance. Unanswered questions, like what elemental composition makes one type of glass stronger than another, or why certain mixtures produce more desirable mechanical traits, drive the promising future of glass science and modern technology as a whole. The pace of modern science innovation is thus closely associated with the advancement of glass science.

Soda-Lime Silicate Glass

Of all the glass composition families, soda-lime silicate (SLS) glass remains the most prevalent and instrumental type of glass. Since SLS is generally inexpensive, chemically durable, and relatively easy to form, it is commonly available in the commercial, automotive, and construction industries as interior and exterior glazing (windows, wall coverings, doors, mirrors, etc.), windshields and rear-view mirrors for automobiles, glass containers for food and beverage, vending machines, oven doors, solar panels, etc. At the core of a SLS glass, its backbone structure is composed of repeated units of tetrahedral SiO_4 (“silica”) as network formers, where each silicone is connected to four oxygen atoms and each oxygen atom is shared by two silicon atoms, as shown in Figure 1 (Karazi, 2017). The oxygen atoms that take part in connecting the two tetrahedral-type unit cells via the Si-O-Si molecular bond are known as “bridging oxygens.”

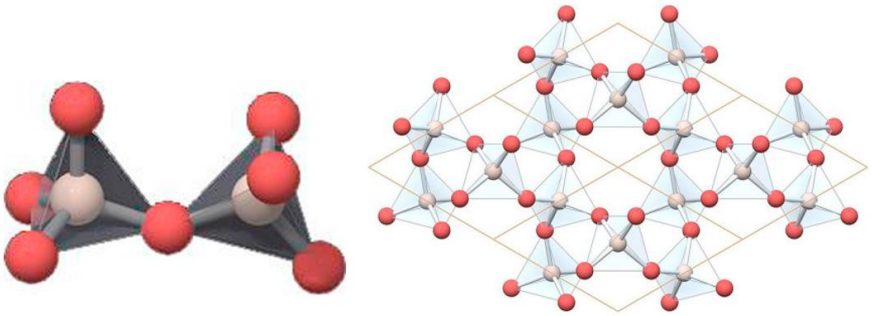

Figure 1. The backbone structure of SLS glass made up of adjacent SiO_4 tetrahedral-type unit cells network formers *(Source: Karazi, 2017).*

The continuity of SLS network is disrupted by the addition of network modifiers, including a majority of Na_2O ("soda") and CaO ("lime") with small amounts of MgO and Al_2O_3, as demonstrated in Figure 2. Hence, "non-bridging oxygens" are introduced, where the initial bridging oxygen of Si-O-Si molecular bond is broken into $Si\text{-}O^-$ fragments upon the addition of positively charged cations. This serves to change the bonding characteristics and network connectivity of the glass structure to further exhibit desired traits for specific properties and application requirements (Karazi, 2017). While the chemical composition of soda-lime silica glass can vary greatly depending on the commercial needs, a typical composition for a SLS glass is 73 wt% SiO_2, 15% Na_2O, 7% CaO, 4% MgO, and 1% Al_2O_3 (Karazi, 2019).

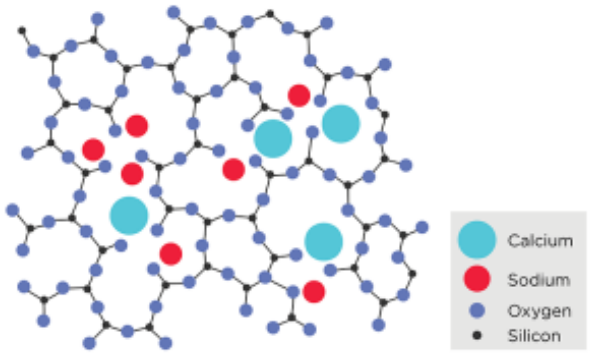

Figure 2. The addition of network modifiers creates discontinuity in SLS glass to enhance desired traits for specific properties and application requirements *(Source: Mauro, 2019).*

The most common production process for SLS glass is the float glass process, originally developed by Pilkington Brothers in 1959 (Haldimann, 2008). More than 85% of the global production of float glass is used for construction applications (Achintha, 2016). For the float glass process, the ingredients (silica, lime, soda, etc.) are first blended with a cullet (recycled broken glass) and then heated up to 1600ºC in a furnace to form molten glass (Achintha, 2016). It will then be fed onto the top of a molten tin bath, where the flat glass ribbon of uniform thickness is produced by flowing molten glass on the tin bath under controlled heating (Achintha, 2016). Upon slow cooling, the tin bath then undergoes annealing with further controlled gradual cooling (Achintha, 2016). The thickness of the glass can be adjusted by altering the speed at which the glass ribbon moves into the annealing lehr (Achintha, 2016). The schematic diagram of the float glass production process is illustrated in Figure 3.

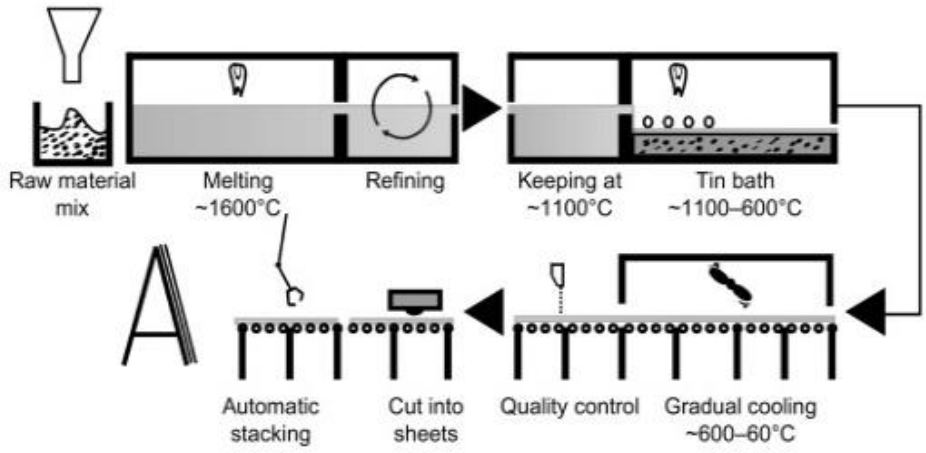

Figure 3. Schematic diagram of the float glass production process *(Source: Achintha, 2016).*

Depending on the chemical composition and the production method, SLS glass embraces distinct mechanical, thermal, and electrical properties. Generally, the density of a SLS glass ranges from 2.45 to 2.60 g/cm^3 (Seward, 2005). SLS undergoes an increase in viscosity with decreasing temperature, thus allowing for operations with high precision requirements (Sanders). The Young's modulus for the glass is typically 68-75 GPa, while its tensile strength is 31-35 MPa, and

its yield strength is around 30-35 MPa (Ashby, 2013). Although SLS glass is a poor thermal insulator with a thermal conductivity of 0.7-1.3 W/m·K, the glass has good electrical insulating properties with a high electrical resistivity of 7.94×10^{17} to 7.94×10^{16} μohm·cm (Ashby, 2013).

Glass Transition Temperature

The glass transition temperature, T_g, is one of the most important factors that give rise to the definition to glass and adds intricacy to the material. Unlike any other crystalline solids, glass do not have a distinct melting point. Since glass are not held together by atoms in an ordered identical crystalline shape, the chemical bonds within glass break over a range of temperature that is denoted as **glass transition temperature.** The glass transition temperature for soda-lime silicate glass is around 500°C to 620ºC depending on the specific chemical composition.

The glass transition temperature range also plays a crucial role in the formation of glass. The volume-temperature diagram for glass in Figure 4 describes the mechanism of glass formation. When a liquid is cooled below its freezing temperature (depicted by *a* to *b* in Figure 4), the transformation phase into super-cooled liquid state takes place to establish a meta-stable equilibrium (*c*). Two different mechanisms could take place, where:

(i) the kinetic driving forces dominate, leading to favorable conditions for nucleation and crystal growth that further allows crystallization (*c, d,* and *e*) to occur, upon which molecular diffusion drives the conversion from liquid to crystal, or

(ii) the thermodynamics driving forces govern the first-order phase transition (*c* and *f*), guided by sufficiently rapid cooling rate, where high viscosity and low molecular mobility results in discontinuity in enthalpy, entropy, and volume.

The latter phenomenon further gives rise to the **glass transition region** as the departure from the super-cooled liquid started to take place, allowing for glass to form. Depending on the cooling rate, the structure of glass differs greatly. Slower cooling rates enables more time for rearrangement in the structure (*b, c,* and *h*), thus the resulting glass has higher density and lower volume. On the contrary, faster cooling rates (*b*, *c*, and *g*) lead to a less compact glass with more open spaces. Fictive temperature, T_f, determined by the intersection between the super-cooled liquid line and the extrapolated glass line, is an approximate concept that indicates the temperature at which super-cooled liquid is instantly frozen into glass (Varshneya, 2019). Hence, fast-cooling glass has higher fictive temperature than slow-cooling glass. Over time, glass continues to relax to super-cooled liquid, transitioning from the *b-c-g* line for fast-cooling glass and *b-c-h* line for slow-cooling glass to the *b-c-f* line.

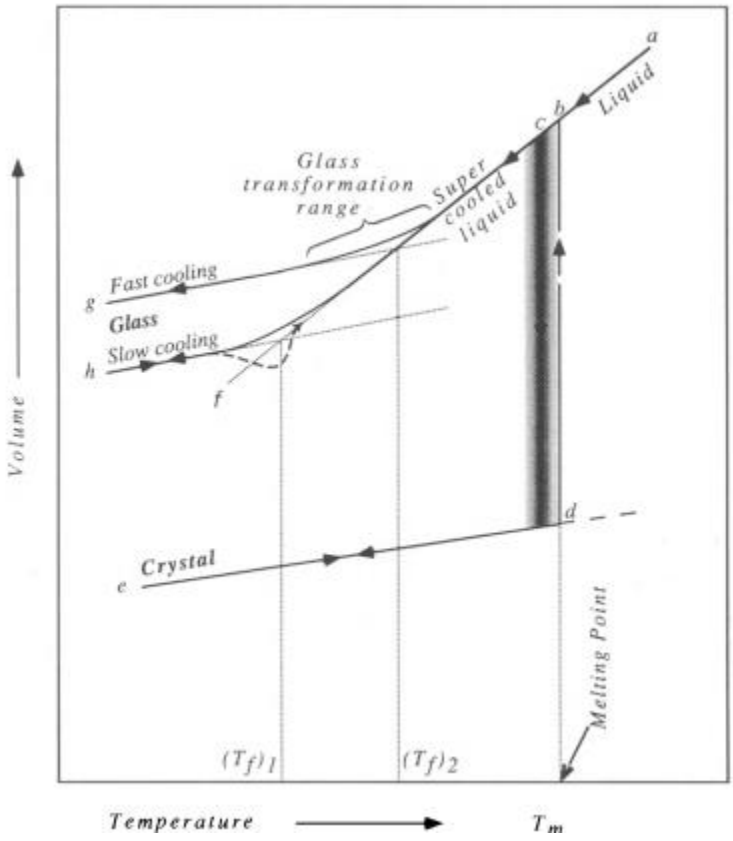

Figure 4. The volume-temperature diagram for glass-forming liquid *(Source: Varshneya, 2019).*

Glass can be reheated to transition back to the super-cooled liquid state. Upon reheating, glass follows the dashed line demonstrated by Figure 4 to move up the curve and transitions back to the super-cooled liquid state, instead of retracing its old path up the transition region, thus explaining the non-equilibrium definition of glass (Varshneya, 2019). As a result, its fluidity increases, yet all other physical appearance remains unchanged.

Annealing Glass

Annealing of glass is a heat treatment process that alters the physical and sometimes chemical properties of a material with the goal to relieve any residual internal stresses retained from manufacturing. It requires initially heating up the glass objects to its annealing temperature, where the viscosity of the glass reaches 10^{13} Poise, and then slowly cooling hot glass objects in a controlled manner until it passes its strain point temperature, where the viscosity is $10^{14.5}$ Poise. The typical annealing temperature range for soda-lime silicate glass is approximately 500°C. In this phase, glass is not sufficiently hard for external deformation, but it is soft enough to relax via microscopic flows in response to internal stresses. The time required for the annealing process depends on the chemical composition of the glass and the thickness of the sample. At the annealing point, stress typically relaxes within several minutes, while at the strain point, stress relaxation could take several hours (Vogel, 1994). It is crucial to allow for enough time for the temperature to be even throughout the system so that the glass sample can be heat-soaked and stress relaxation can be performed adequately.

Vickers Hardness Test

One of the most prevalent methods for evaluating the micro-hardness of glass is the Vickers hardness test, developed by Robert L. Smith and George E. Sandland at Vickers Ltd (Smith and Sandland, 1922). The fundamental principle of the Vickers test is to examine the various levels of deformations of the material upon the introduction of a square pyramid diamond indentation, as depicted in Figure 5. The size of the indentations is generally of the order of a few microns under 5 to 1,000 g loads (Varshneya, 2019), and the total time for indentation implementation from gradually descending the load onto the sample surface to generating equilibrium penetration depth is around 15-25 seconds for each measurement.

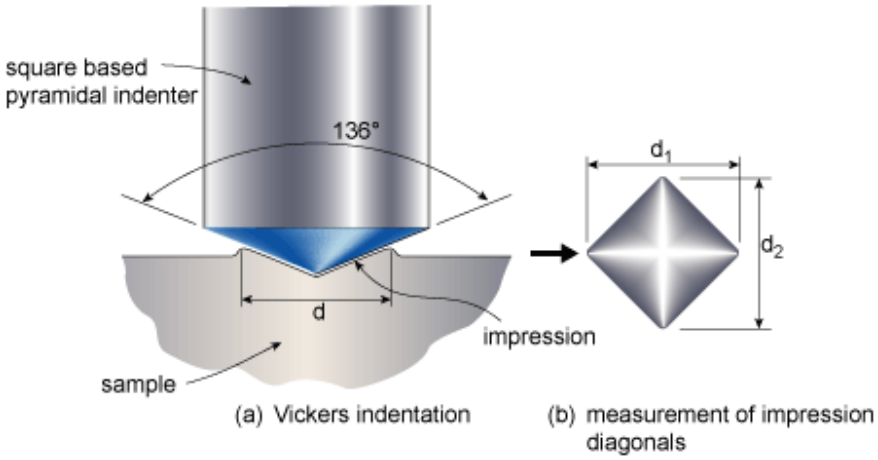

Figure 5. The square pyramid shape geometry for Vickers indentation *(Source: Mathers).*

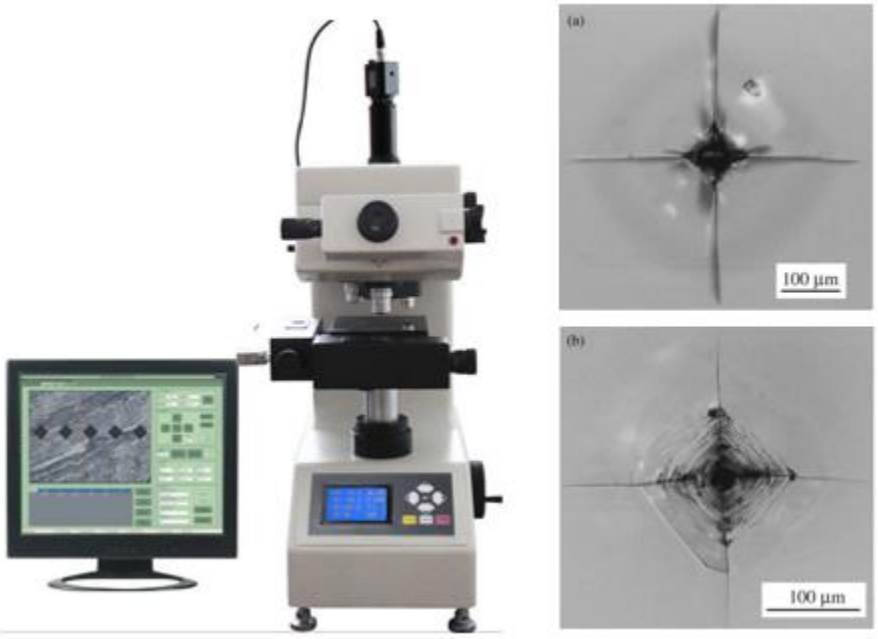

Figure 6. An example of the Vicker hardness tester and the direct view of Vickers indentations on (a) soda-lime glass and (b) borosilicate glass *(Source: DongGuan Sinowon Precision Instruments and Burghard, 2004).*

Once the indentation is introduced onto the glass sample, glass experiences elastic compression and shear driven by the hydrostatic and shear component (Varshneya, 2019). Upon the elastic limit, the balance of hydrostatic component permanently densifies the glass, whereas the shear stress component leads to plastic deformation (Varshneya, 2019). When the indenter is withdrawn, a slight shrinkage of the impression size occurs, implying the recovery from the elastic deformation. Cracking from diagonals develop upon applied force of indentation and is an attainment of fracture strength. Figure 7 and 8 shows the different layers of deformation that glass undergoes from Vickers indentation and the resulting cracks on the glass surface.

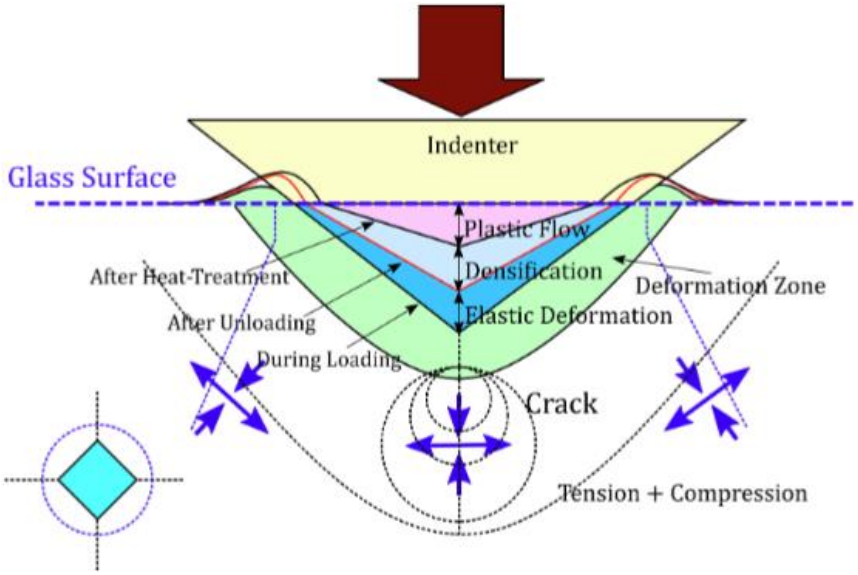

Figure 7. Different layers of deformation in glass upon the introduction of Vickers indentation *(Source: Mauro, 2019).*

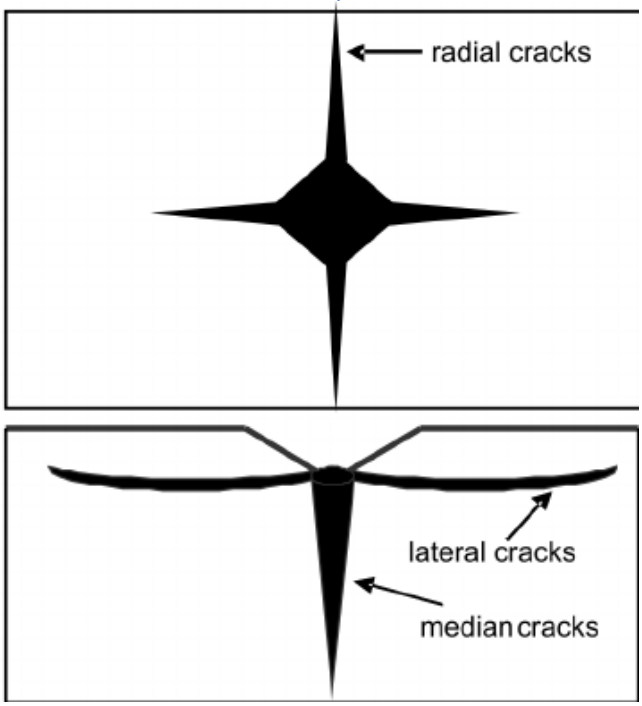

Figure 8. The resulting cracks on the glass surface after Vickers indentation is introduced *(Source: Chorfa, 2010).*

For a standard Vickers hardness test, the micro-hardness behaviors of the material can be determined based on the following formula,

$$A = \frac{D^2}{2\sin(\frac{136^o}{2})} \approx \frac{D^2}{1.8544}$$

$$Vickers\ Hardness\ Number\ (VHN) = \frac{Force}{Area} = \frac{2Fsin(\frac{\theta}{2})}{D^2} = 1.8544\frac{F}{D^2}$$

where A is the surface area of the resulting indentation in mm^2, D is the average diagonal of the impression in mm, F is the force applied in kg, and θ is the included angle of the Vickers pyramid ($\theta = 136^o$) (ASTM E384).

Chapter 2

Experimental Methods

Sample Preparation

The samples used for the experiment were 4-millimeters float SLS glass supplied by PPG Industries Works #6 plant (now Vitro Architectural Glass, Carlisle, PA) and 1-millimeters thick panels provided by Asahi Glass Co. (Japan). Due to the floating production process of SLS glass (as described in Chapter 1), the glass samples were distinguished between their "tin side" (the glass surface that came in contact with the molten tin bath) and "air side" (the opposite surface that was in contact with air). All experimental analyses were made on the air side of the glass to rule out any complications about the chemical compositions at the surface level. The samples were cut into small rectangular pieces of 3.5" x 1.5". They were sonicated with ethanol on top of careful rinsing with DI water, ethanol, and acetone and were exposed to an ozone environment for 15 minutes.

For this thesis, the self-healing properties of SLS glass will be examined for its correlation with two instrumental parameters, namely (i) the annealing conditions and (ii) the pre-treatment effects with water. Hence, the sample preparations prior to thermal healing executions for these two experimental concepts differ slightly, yet the thermal healing procedures should be identical.

Experiment #1: Examine the effects of annealing conditions and thermal treatment temperatures on the self-healing ability of SLS glass

To observe the effects of annealing conditions on thermal treatment, three 4-mm PPG SLS glass samples were annealed at different temperatures (550°C and 570°C) for two hours with a ramping condition of 15°C per minute and were allowed to cool for one day. Vickers indentation was then introduced onto the "air side" of the glass samples at 500-gram force for 15 seconds. Each sample contains four indentations equally spread out on the glass surface. After the samples were carefully cleaned with DI water, ethanol, and acetone, sonicated with ethanol, and exposed to an ozone environment for 15 minutes, thermal treatment was carried out in the glass transition temperature range (500°C and 600°C) for a time span of 12, 24, 36, and 48 hours. The image of the Vickers indentation for each glass sample was captured on microscope and labelled accordingly. ImageJ software was used to analyze the length of the radial cracks before and after the thermal healing process. A list of experimental conditions executed for the study of the relationship between annealing conditions and thermal treatment is summarized in Table 1.

Table 1. Summary of experimental conditions for the study of annealing temperature and thermal treatment temperature effects on thermal healing abilities

Experimental Conditions for the Relationship Between Annealing Conditions and Thermal Healing Abilities							
Glass Provider	**Glass Size**	**Glass No.**	**Indent. No.**	**Crack No.**	**Pre-Treatment**	**Thermal Treatment**	**Timespan (Hours)**
PPG	4mm	1	1	1, 2, 3, 4	Annealed at T = 570°C for 2 hours	Thermal treatment at T = 600°C	12, 24, 36, 48
			2	1, 2, 3, 4			
			3	1, 2, 3, 4			
			4	1, 2, 3, 4			
PPG	4mm	2	1	1, 2, 3, 4	Annealed at T = 550°C for 2 hours	Thermal treatment at T = 600°C	12, 24, 36, 48
			2	1, 2, 3, 4			
			3	1, 2, 3, 4			
			4	1, 2, 3, 4			
PPG	4mm	3	1	1, 2, 3, 4	Annealed at T = 550°C for 2 hours	Thermal treatment at T = 500°C	12, 24, 36, 48
			2	1, 2, 3, 4			
			3	1, 2, 3, 4			
			4	1, 2, 3, 4			

Experiment #2: Evaluate the pre-treatment effects with water of SLS glass on its self-healing properties

The understanding of the pre-treatment effects with water on SLS glass can be done by executing different pre-treatment procedures on the glass sample before thermal healing. Two 1-mm Asahi SLS glass samples were annealed at 570°C for two hours with a ramping condition of 15°C per minute and were allowed to cool for one day. One sample was pre-treated with 55% Relative Humidity (RH) for 1.5 hours, while the other did not undergo any pre-treatment procedures. Each glass sample was then introduced with ten Vickers indentation at 500-gram force for 15 seconds. The glass samples were then rinsed with DI water, ethanol, and acetone, sonicated with ethanol, and exposed to an ozone environment for 15 minutes. Thermal healing was carried out in the glass transition range at 600°C for a time span range from 8 to 35 hours. The sample radial cracks for each Vickers indentation were captured by the microscope before and after the thermal treatment process to analyze its length on ImageJ software. Table 2 presents all experimental conditions executed for the study of water pre-treatment and thermal healing abilities.

Table 2. Summary of experimental conditions for the study of water pre-treatment and thermal healing abilities

Experimental Conditions for the Relationship Between Water Pre-Treatment and Thermal Healing Abilities							
Glass Provider	**Glass Size**	**Glass No.**	**Indent. No.**	**Crack No.**	**Pre-Treatment**	**Thermal Treatment**	**Timespan (Hours)**
Asahi	1mm	1	1	1, 2, 3, 4	Annealed at T=570°C with no water pre-treatment	Thermal treatment at T = 600°C	8, 18, 35
			2	1, 2, 3, 4			
			3	1, 2, 3, 4			
			4	1, 2, 3, 4			
			5	1, 2, 3, 4			
			6	1, 2, 3, 4			
			7	1, 2, 3, 4			
			8	1, 2, 3, 4			
			9	1, 2, 3, 4			
			10	1, 2, 3, 4			

Asahi	1mm	2	1	1, 2, 3, 4	Annealed at T = 570°C and pre-treated with 55% RH for 1.5 hours	Thermal treatment at T = 600°C	17, 27, 34
			2	1, 2, 3, 4			
			3	1, 2, 3, 4			
			4	1, 2, 3, 4			
			5	1, 2, 3, 4			
			6	1, 2, 3, 4			
			7	1, 2, 3, 4			
			8	1, 2, 3, 4			
			9	1, 2, 3, 4			
			10	1, 2, 3, 4			

Thermal Treatment Conditions

The thermal treatment experimental set-up for all experiments are identical with the only difference being the furnace temperatures. The glass sample was first placed inside a ceramic holder that was then placed on top of the thermocouple inside a sealed furnace system. To start the thermal process, the desired temperature was set for the furnace with a ramping condition of 10^{o}C per minute under dry nitrogen conditions. Typically, it took about thirty to forty minutes for the furnace to reach the temperature range of 500°C to 600°C from room temperature. To simulate the humid environment, 3 L/min of nitrogen gas was then bubbled inside a 5-Liter graduated cylinder filled with water and silicone beads, upon which the saturated water vapor will be produced and fed into the furnace system. The furnace was left running for a specified timeframe depending on the experiments. For the shut-down procedures, the furnace temperature was decreased to room temperature, and the system was allowed to gradually cool down, typically an hour, to reach room temperature. The schematic diagram for the experiment apparatus is presented in Figure 9.

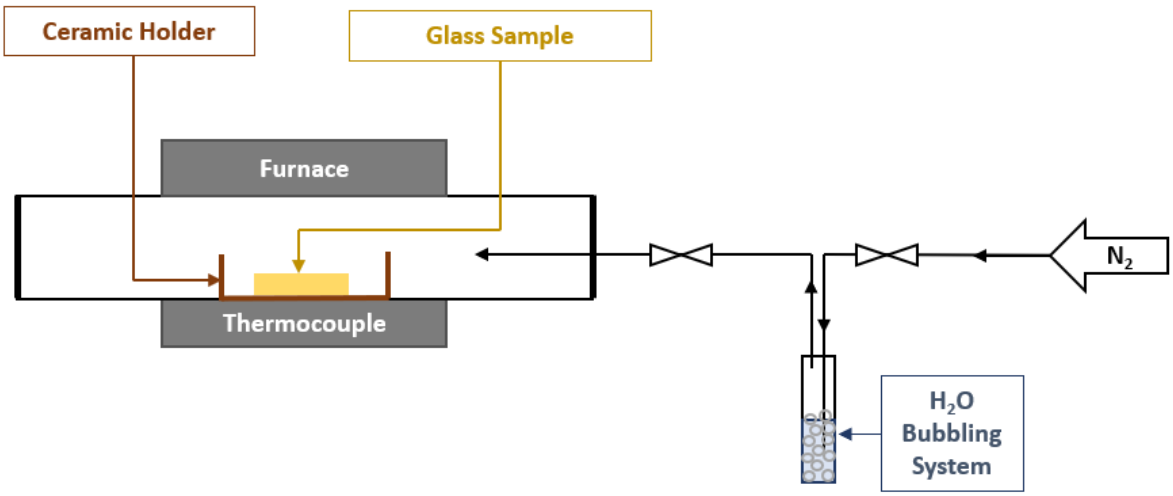

Figure 9. Schematic diagram for thermal treatment apparatus.

Radial Crack Length Measurement

The evaluation of the thermal healing abilities was made by measuring the radial crack lengths of the Vickers indentation from the captured microscope images via ImageJ software, which is a Java-based image processing program developed by the National Institutes of Health and the Laboratory for Optical and Computation Instrumentation at University of Wisconsin (Schneider, 2012). Calibration was executed on a caliper ruler with a known scale, resulting in a standard basis of 3.6376 pixels/micron. This basis was used consistently for all sample measurements.

Each Vickers indentation contains four different radial crack lengths, all of which were labelled accordingly to be measured before and after the thermal healing process was carried out. The radial crack length distance was measured from the corner of the rhombus to the tip of the crack. Figure 10 shows an example of how the radial cracks are measured within ImageJ software.

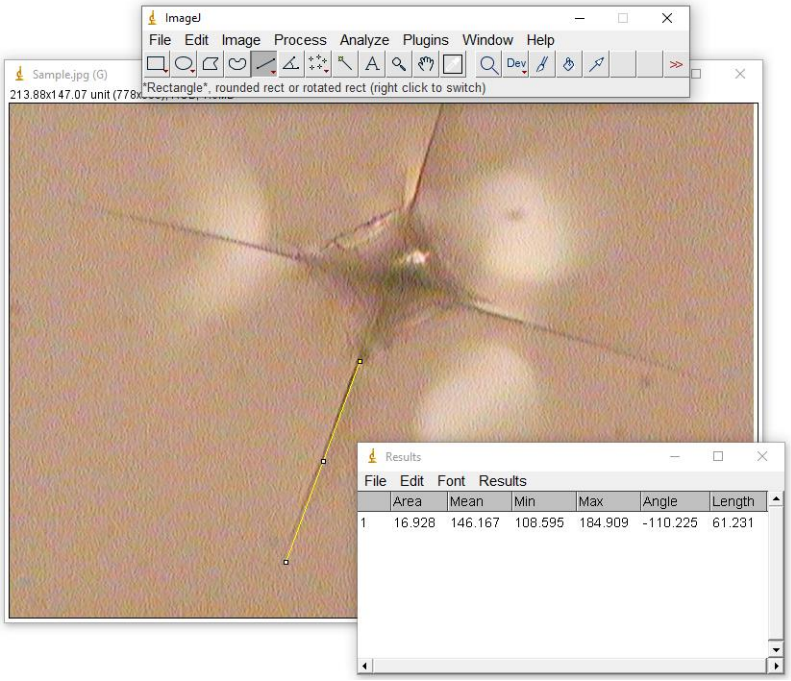

Figure 10. Radial cracks are measured using ImageJ software.

Chapter 3

Results and Discussions

Current Profile

While the self-healing properties are the main subject of study for the thesis, the nature of the experiments studying the annealing conditions effects and the water pre-treatment impacts differ vastly; hence, the results are discussed separately within this section. The qualitative and quantitative results for the experiments are displayed in Table 3-6.

Table 3. Summary of qualitative experimental results for the study of annealing temperature and thermal treatment temperature effects on thermal healing abilities

Experimental Qualitative Results for the Relationship Between Annealing Conditions and Thermal Healing Abilities						
Sample No.	**Crack No.**	**Before Thermal Treatment**	**After 12 Hours**	**After 24 Hours**	**After 36 Hours**	**After 48 Hours**
1	1	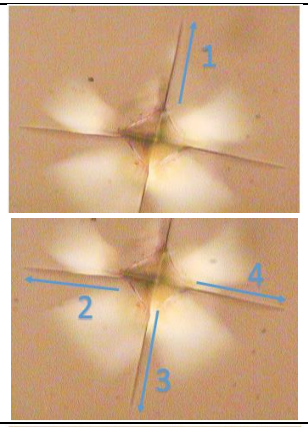	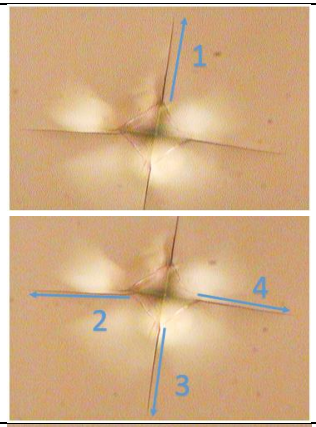	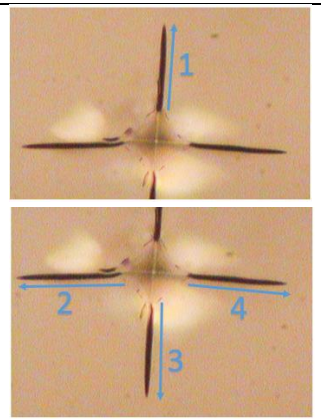	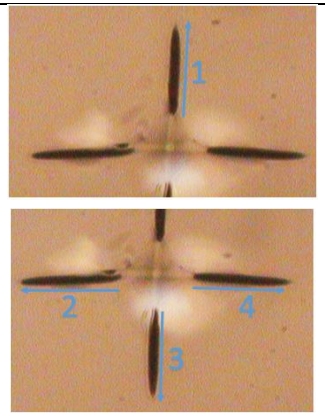	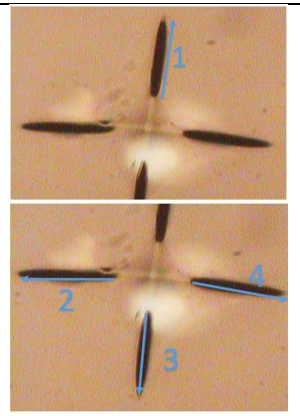
	2	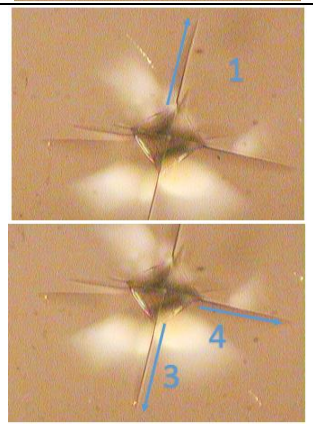	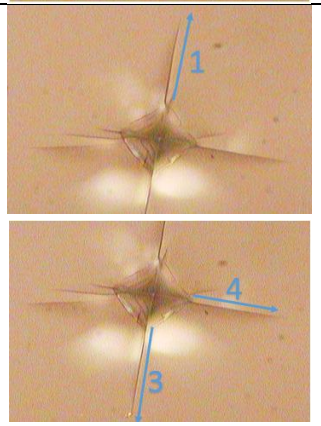	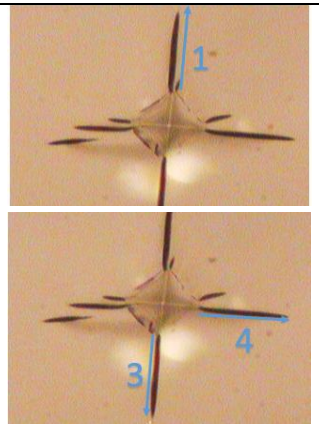	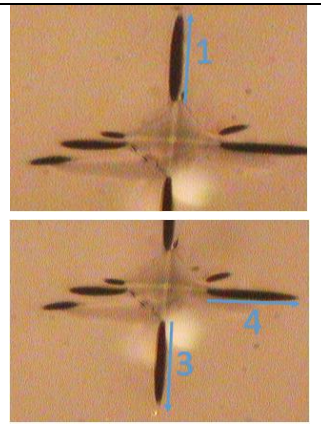	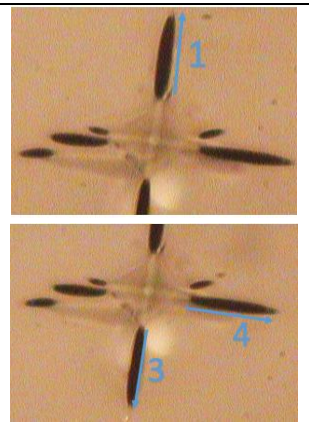

	3	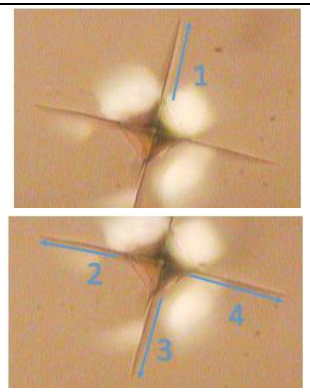	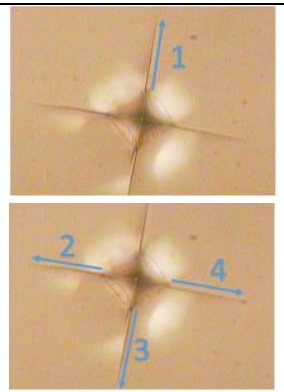	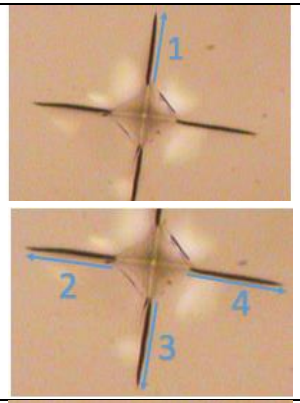	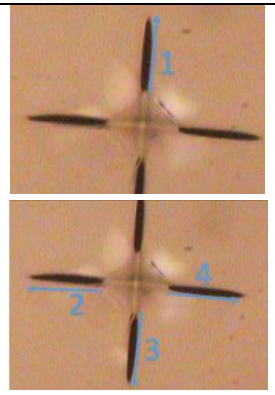	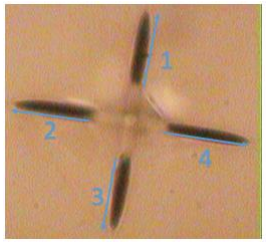
	4	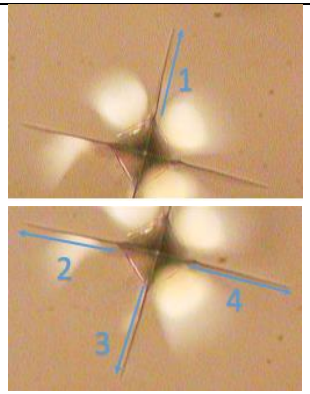	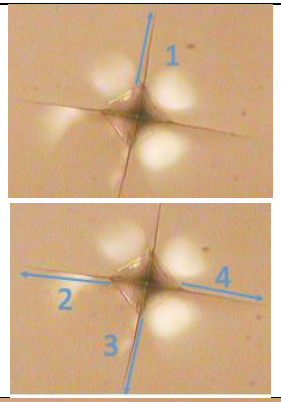	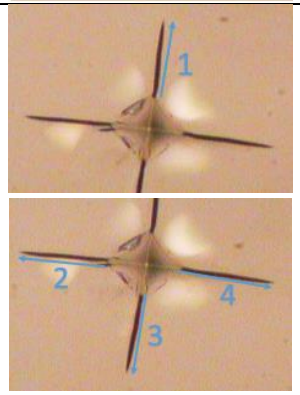	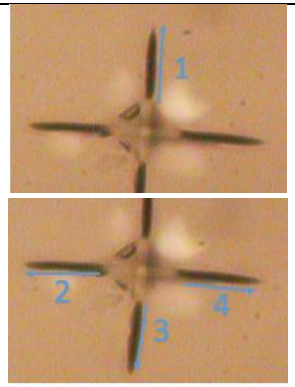	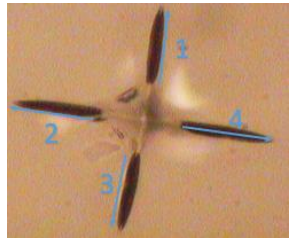
2	1	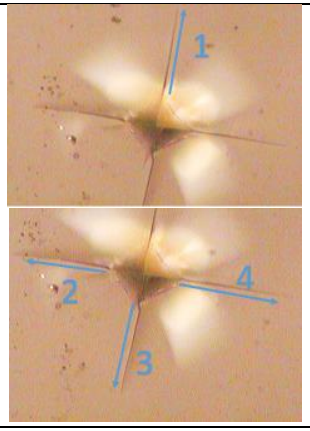	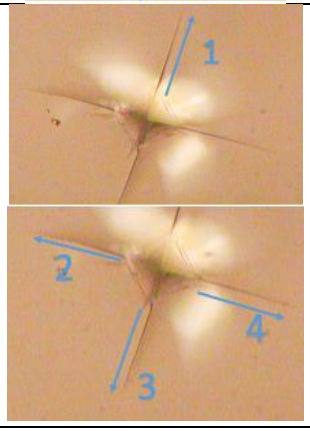	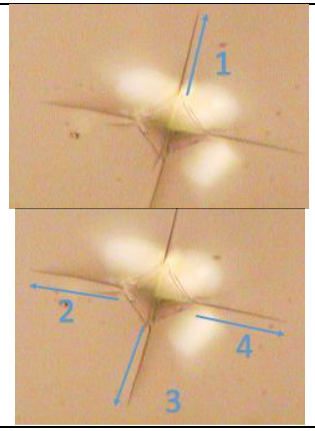	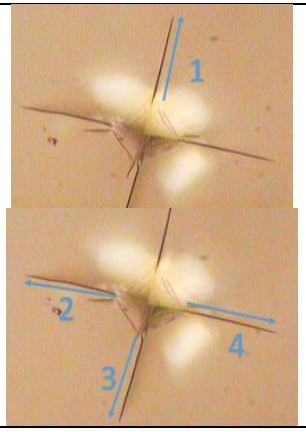	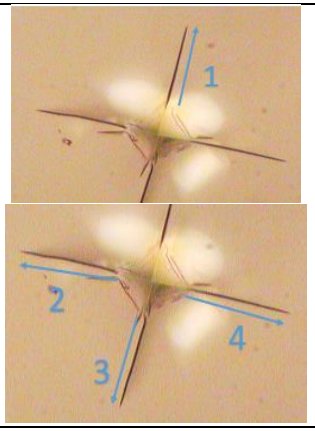

	2	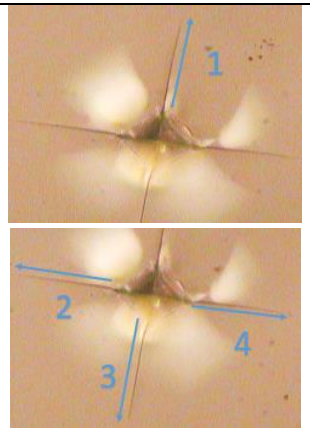	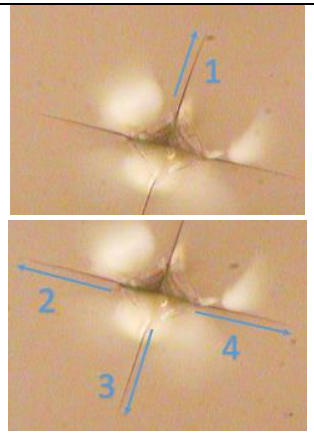	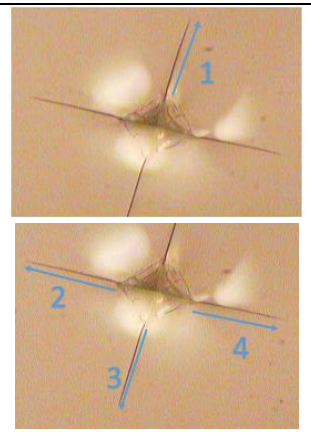	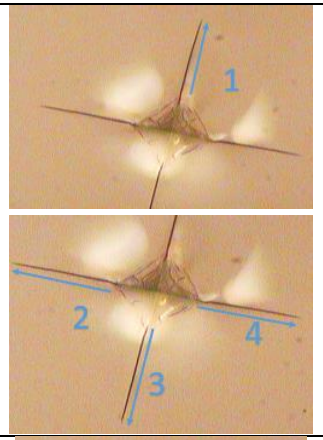	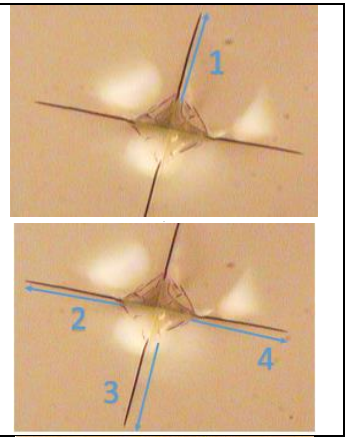
	3	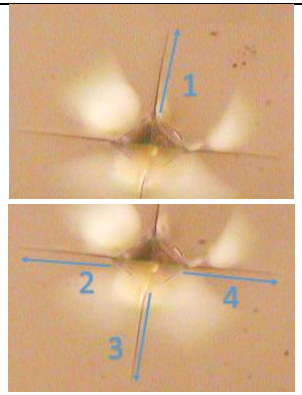	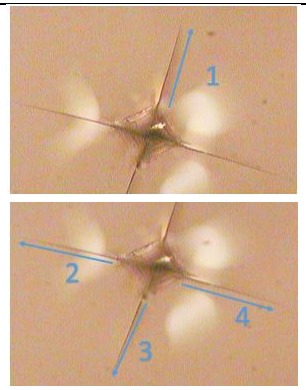	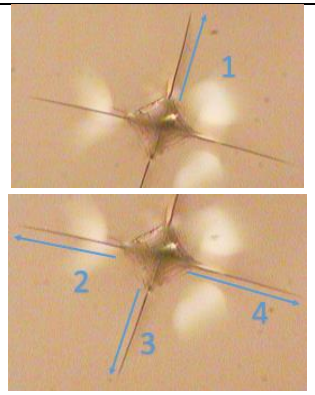	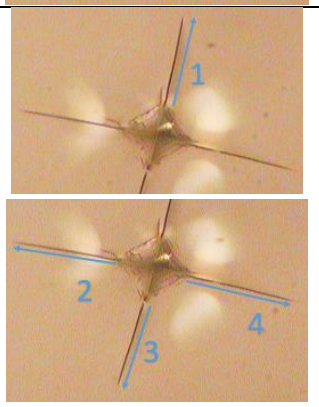	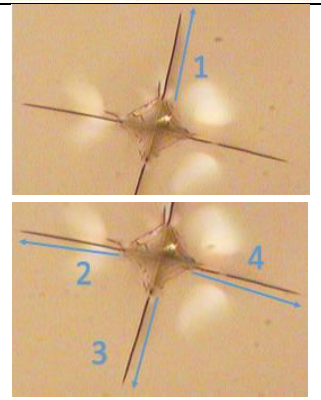
	4	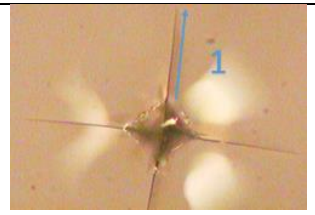	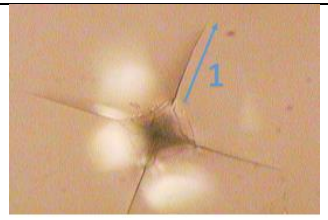	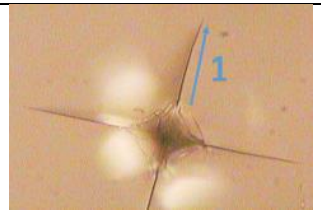	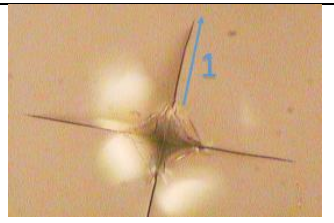	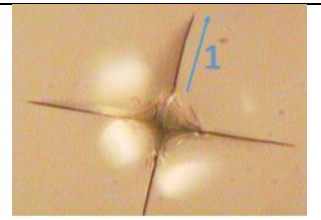

		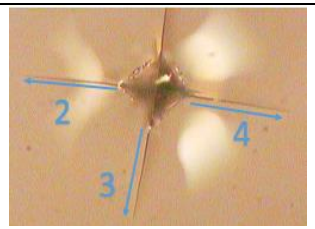	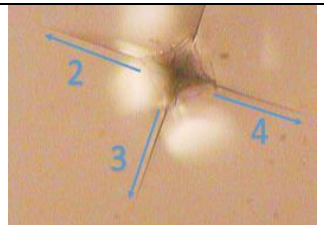	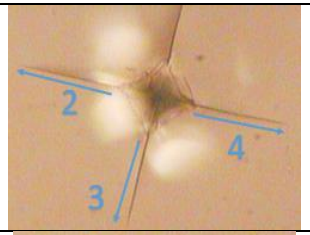	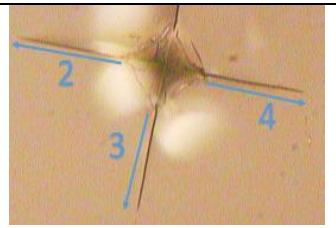	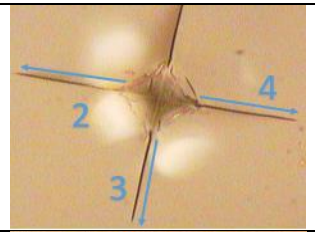
3	1	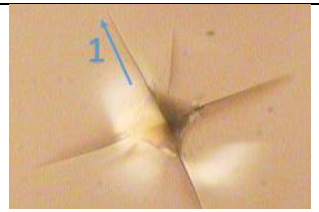 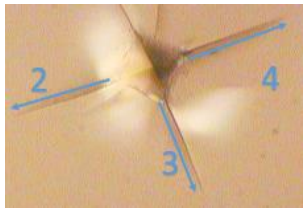	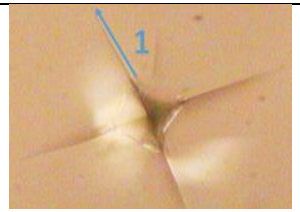 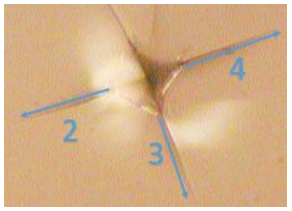	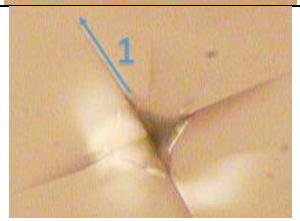 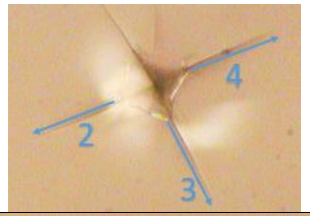	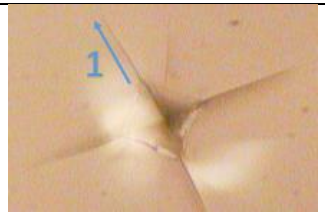 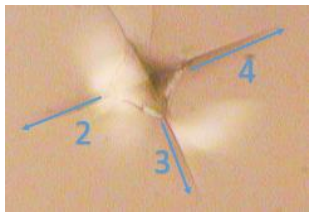	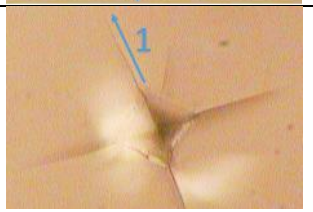 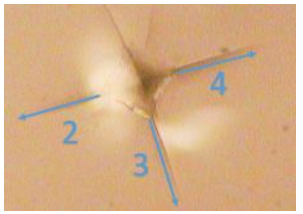
	2	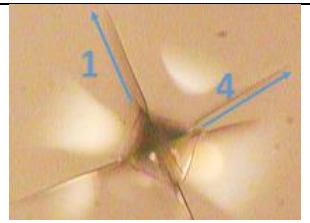 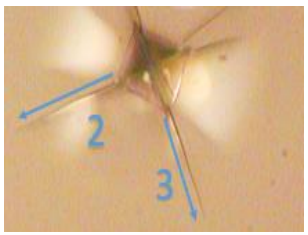	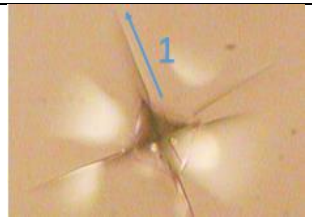 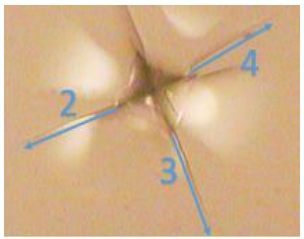	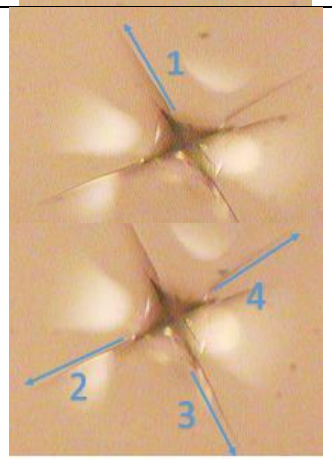	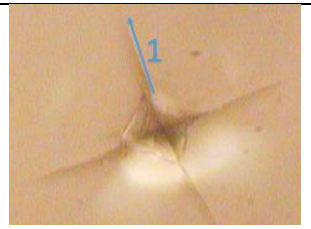 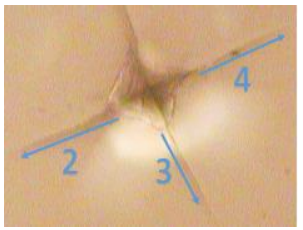	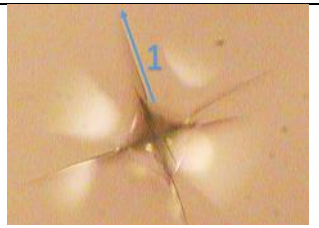 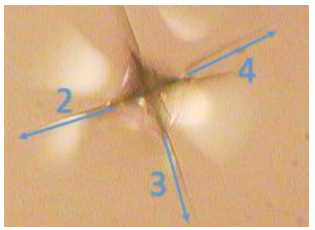

	3	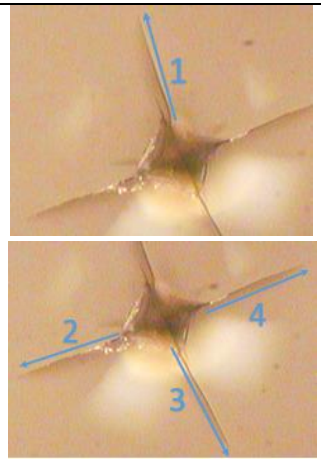	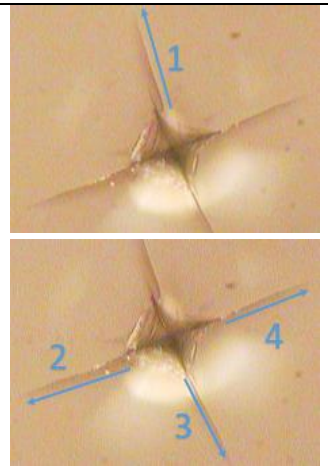	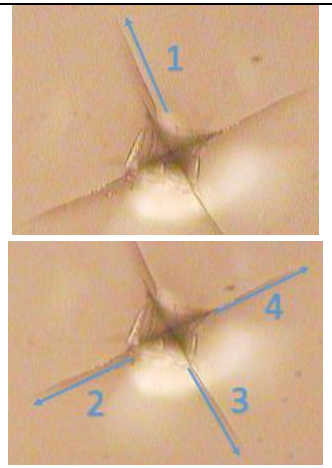	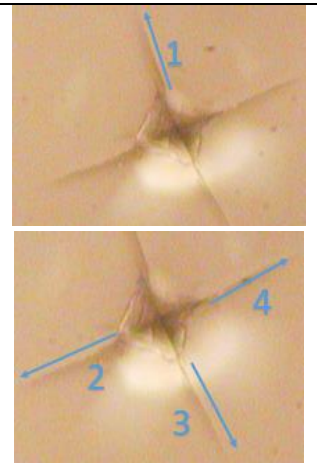	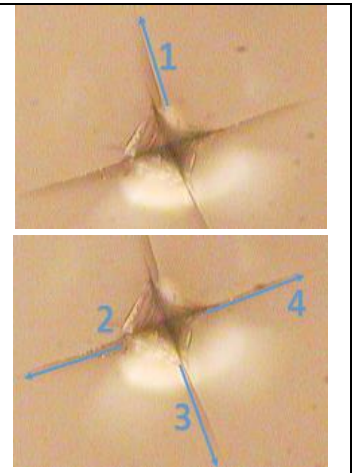
	4	Vickers indentation #4 was not considered because the radial cracks were not evenly distributed due to imprecise execution.				

Table 4. Summary of qualitative experimental results for the study of water pre-treatment and thermal healing abilities

Experimental Qualitative Results for the Relationship Between Water Pre-Treatment and Thermal Healing Abilities					
Sample No.	**Crack No.**	**Before Thermal Treatment**	**After 8 Hours**	**After 18 Hours**	**After 35 Hours**
1	1	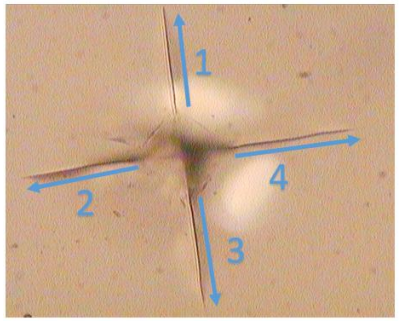	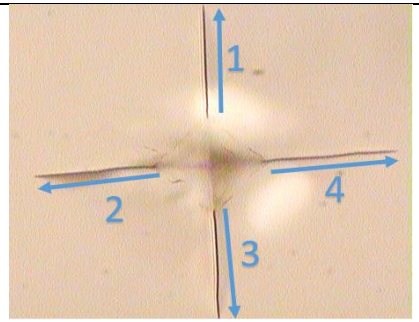	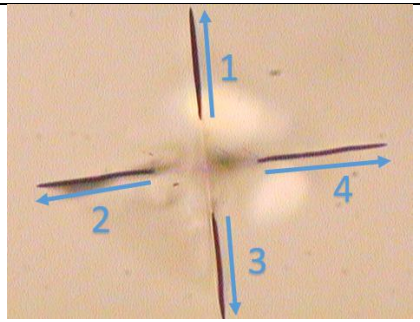	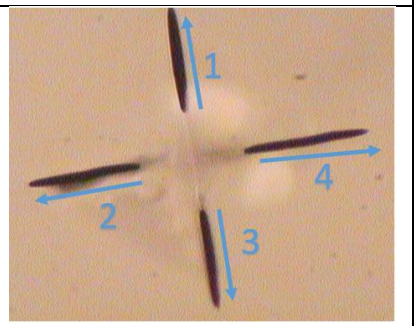
	2	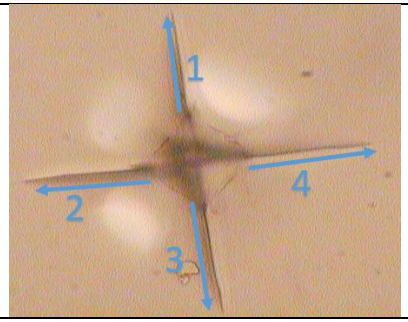	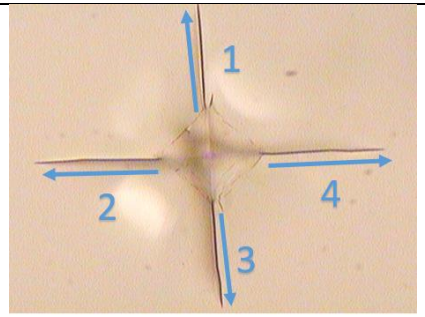	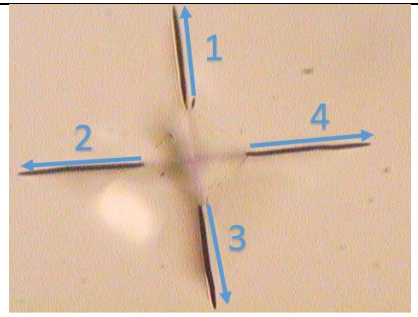	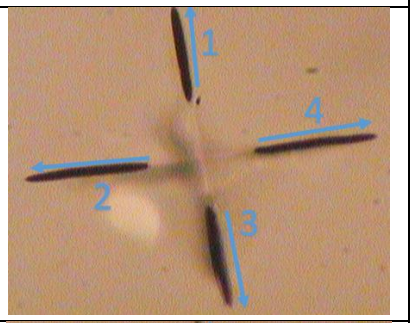
	3	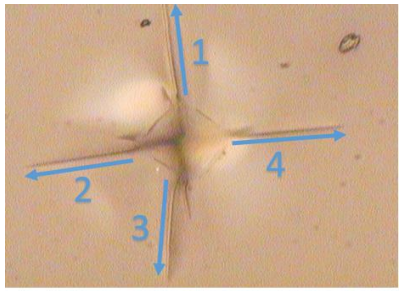	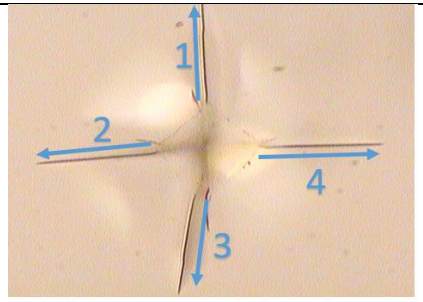	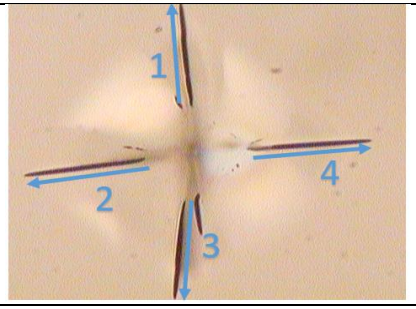	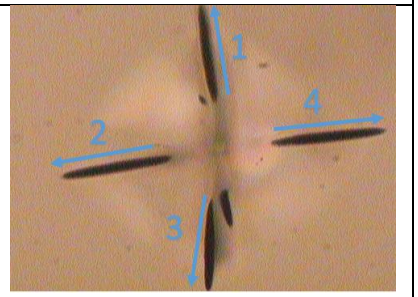

	4	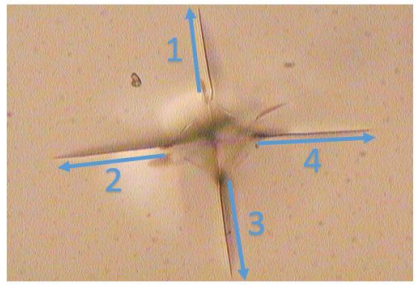 1 2 4 3	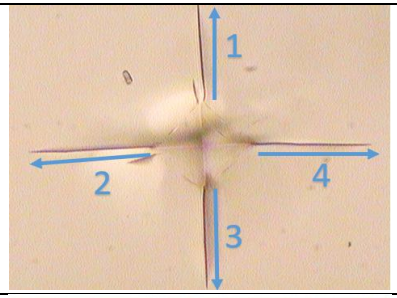 1 2 4 3	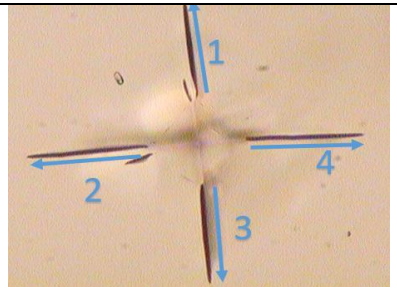 1 2 4 3	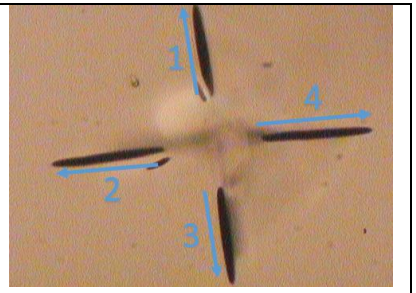 1 2 4 3
	5	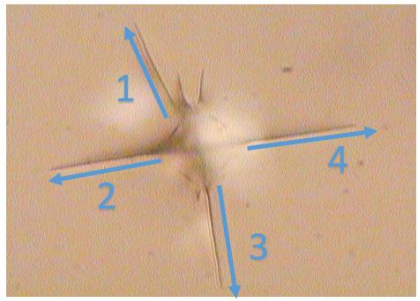 1 2 4 3	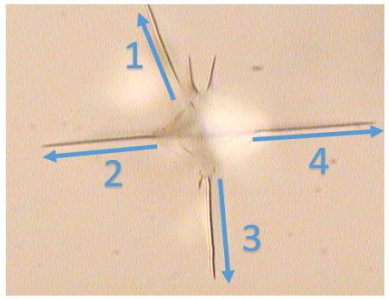 1 2 4 3	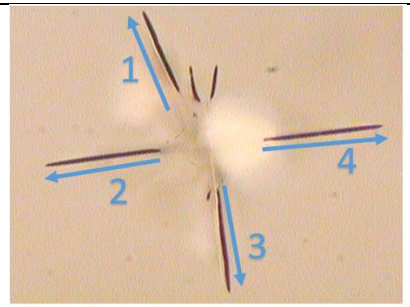 1 2 4 3	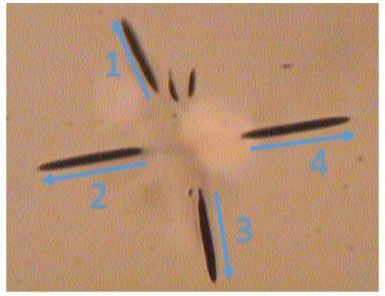 1 2 4 3
	6	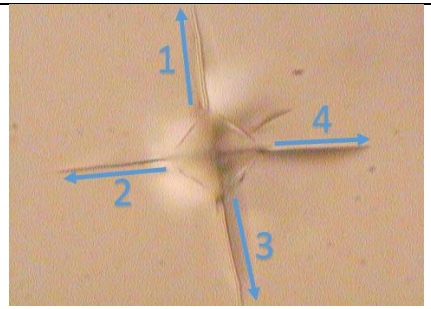 1 2 4 3	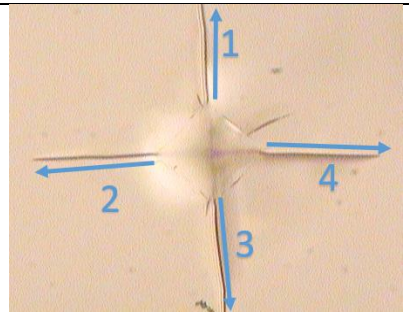 1 2 4 3	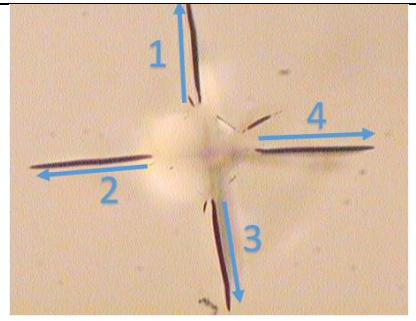 1 2 4 3	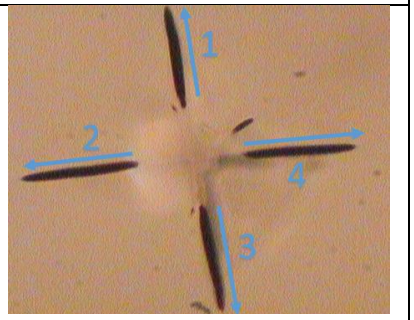 1 2 4 3

	7	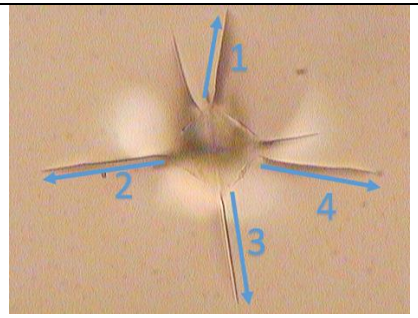 1 2 4 3	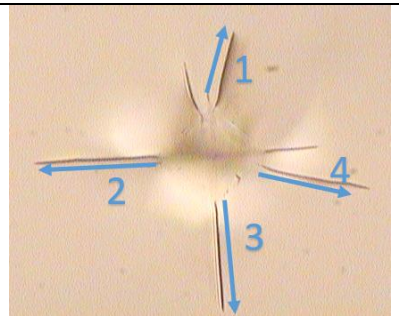 1 2 4 3	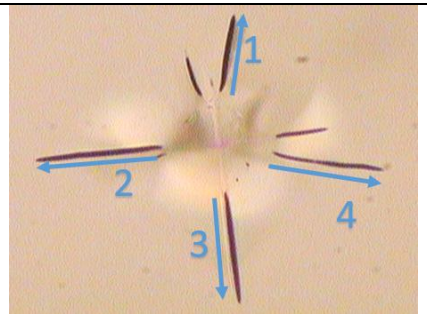 1 2 4 3	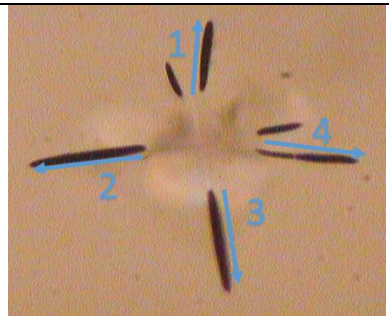 1 4 2 3
	8	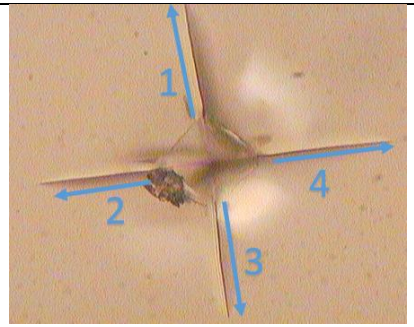 1 4 2 3	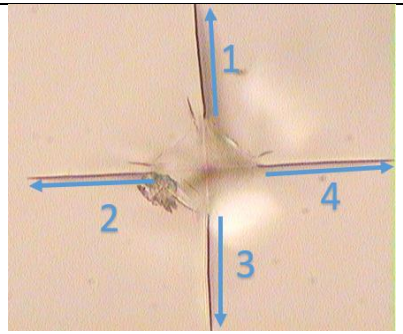 1 4 2 3	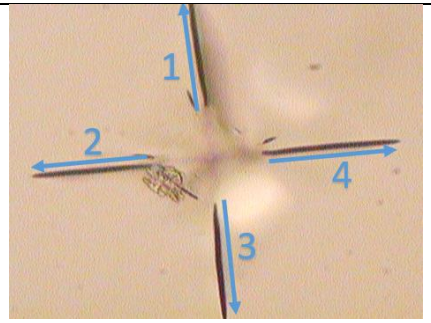 1 2 4 3	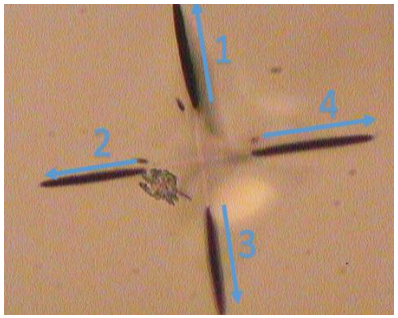 1 4 2 3
	9	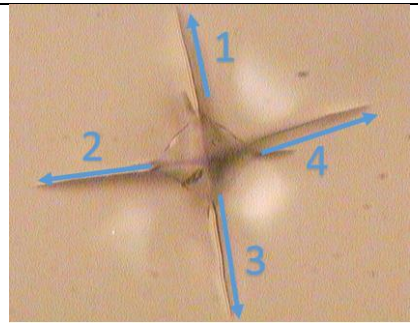 1 2 4 3	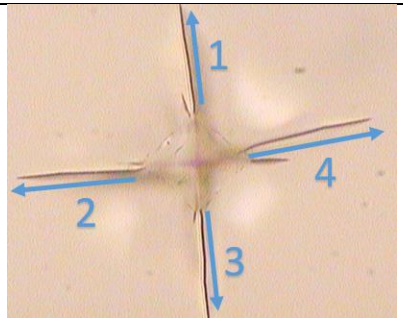 1 4 2 3	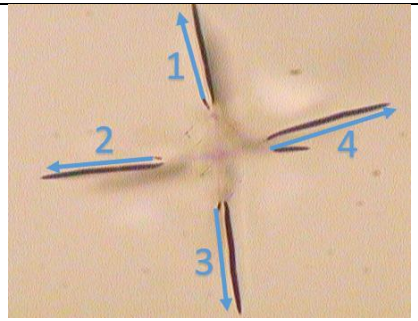 1 2 4 3	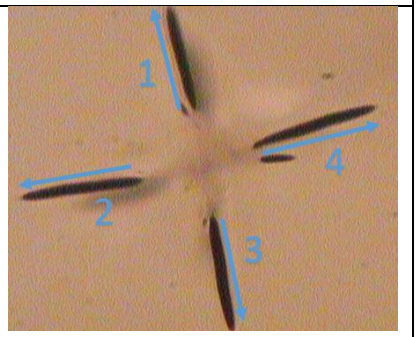 1 4 2 3

	10	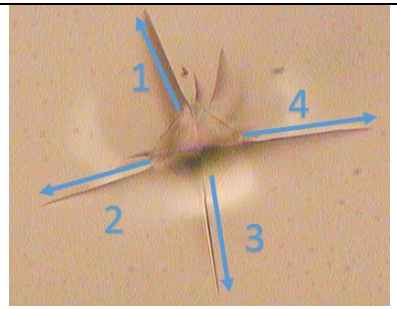	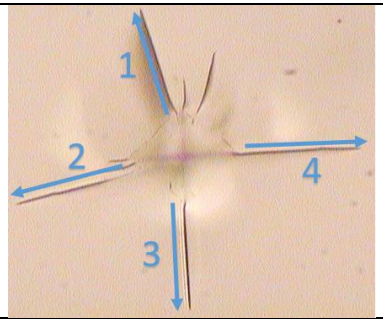	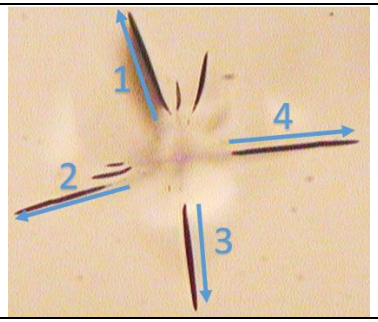	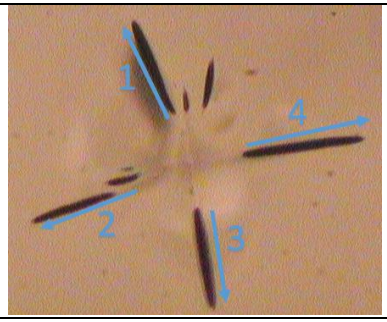
Sample No.	**Crack No.**	**Before Thermal Treatment**	**After 17 Hours**	**After 27 Hours**	**After 34 Hours**
2	1	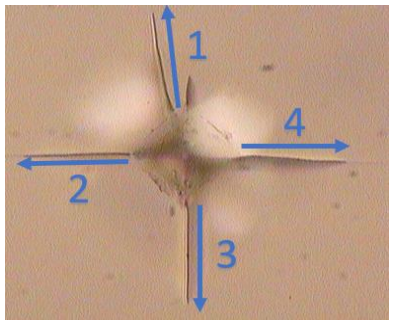	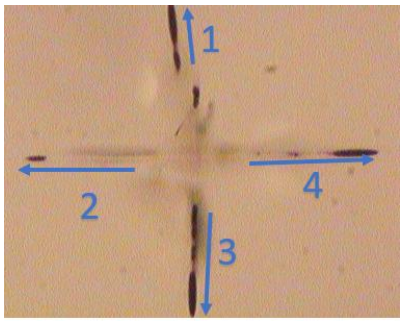	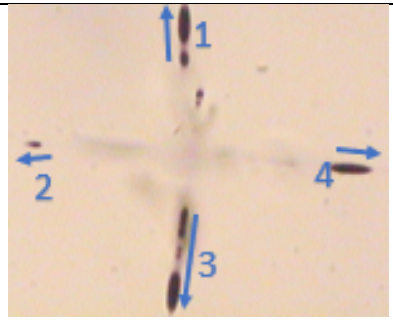	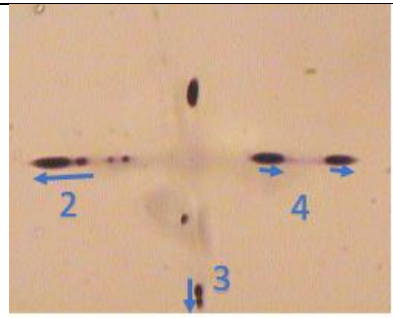
	2	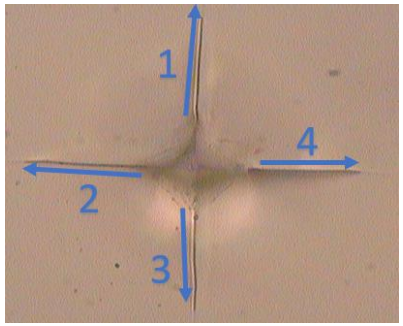	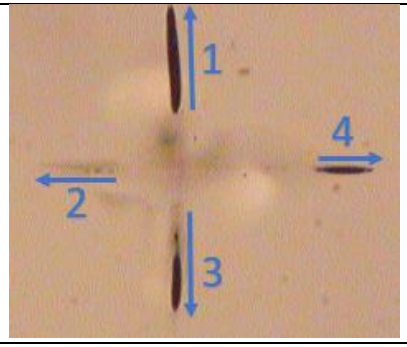	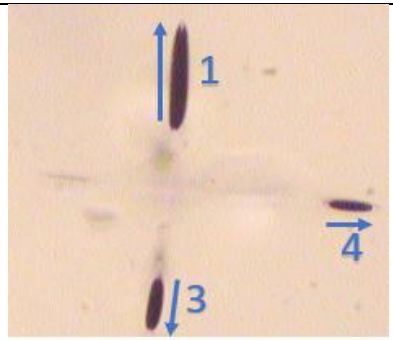	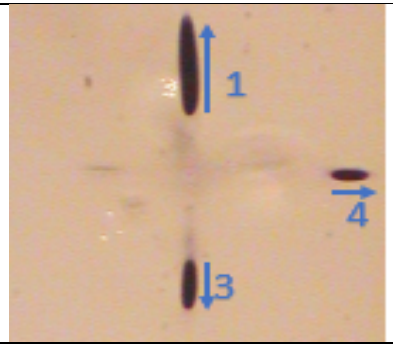

	3	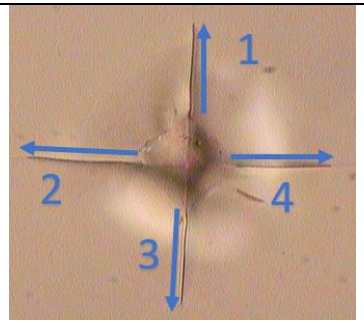 1 2 4 3	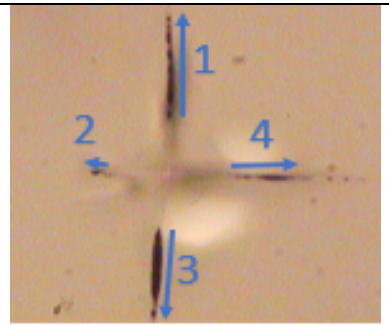 1 2 4 3	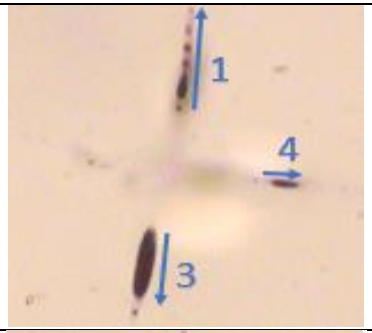 1 4 3	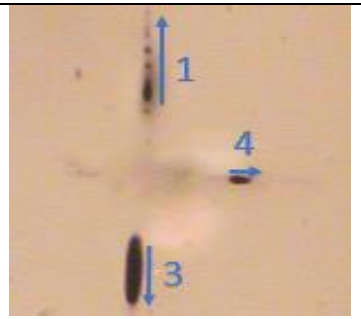 1 4 3
	4	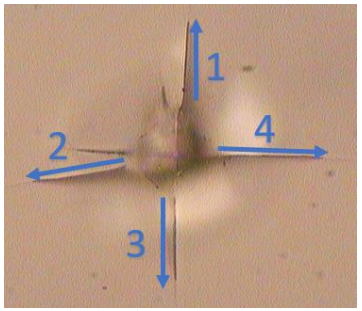 1 2 4 3	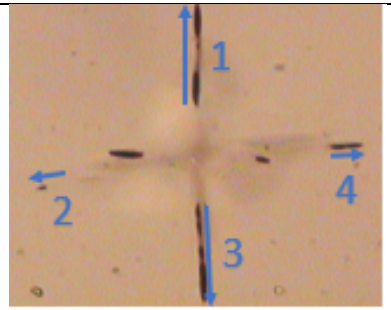 1 2 4 3	 1 2 4 3	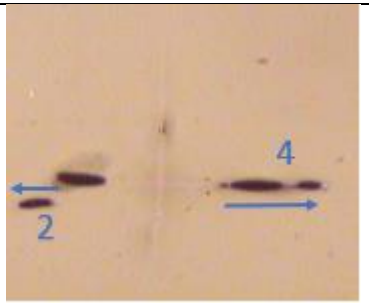 4 2
	5	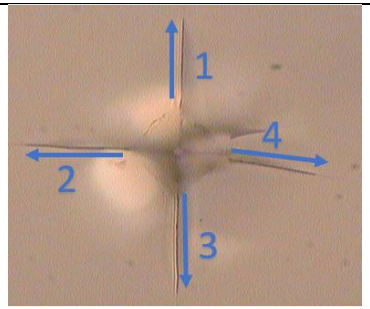 1 4 2 3	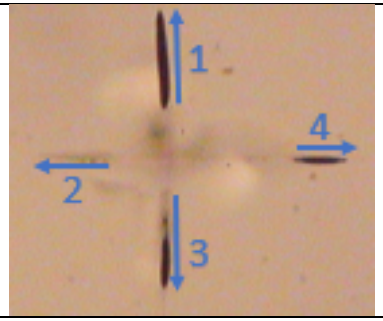 1 4 2 3	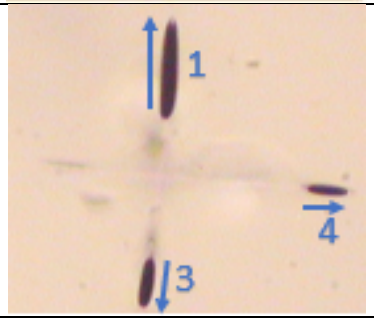 1 4 3	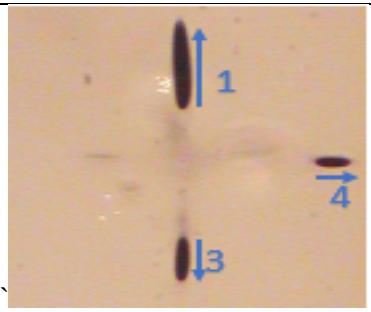 1 4 3

	6	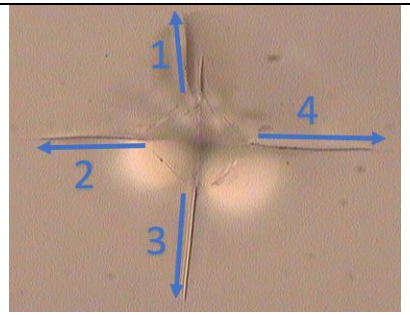 1 4 2 3	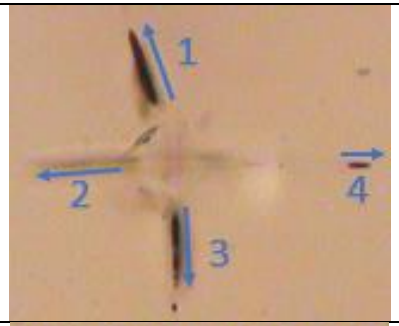 1 2 4 3	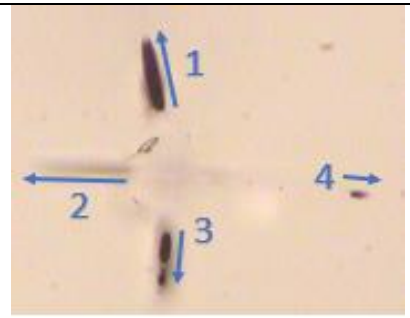 1 4 2 3	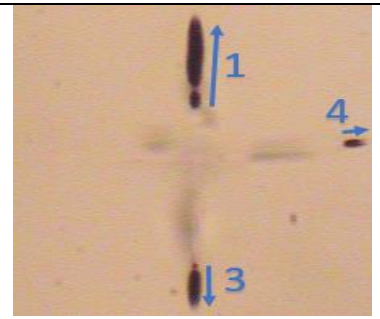 1 4 3
	7	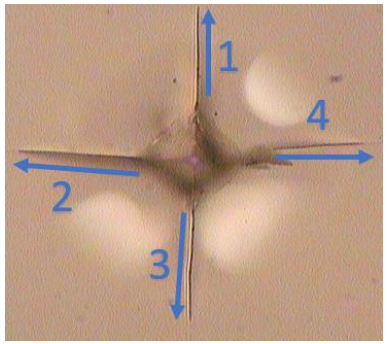 1 4 2 3	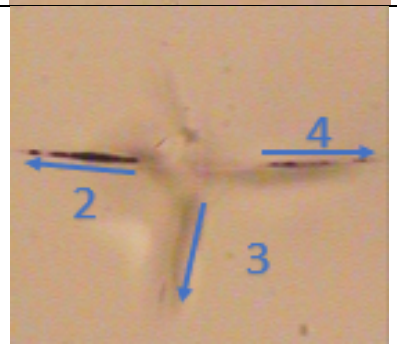 4 2 3	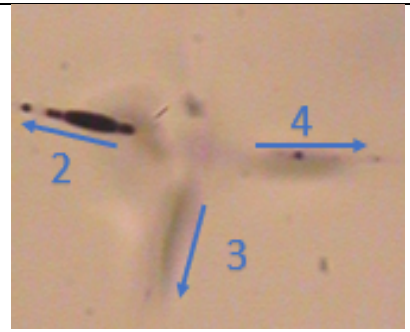 4 2 3	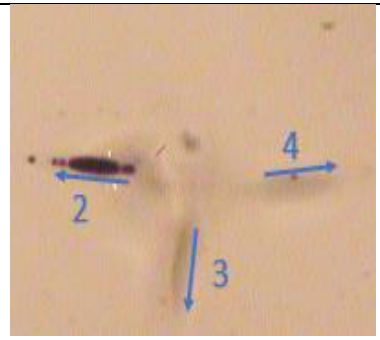 4 2 3
	8	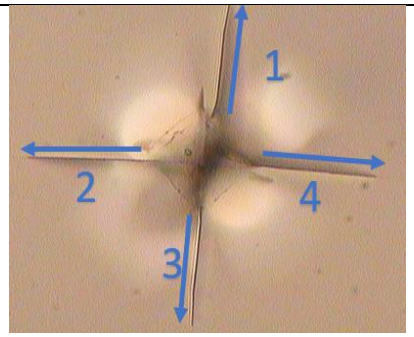 1 2 4 3	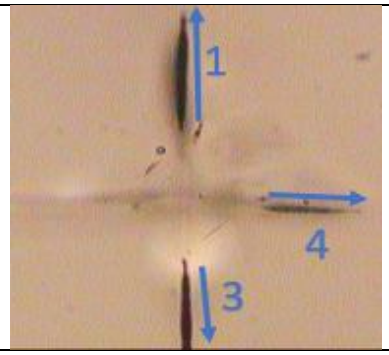 1 4 3	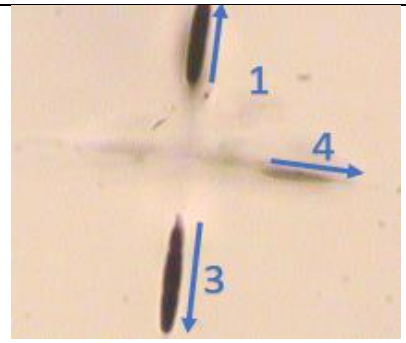 1 4 3	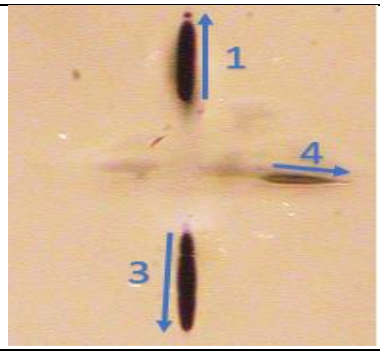 1 4 3

	9	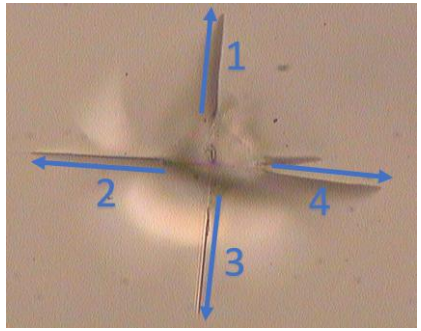 1 2 4 3	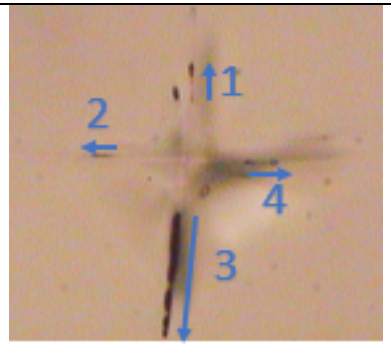 1 2 4 3	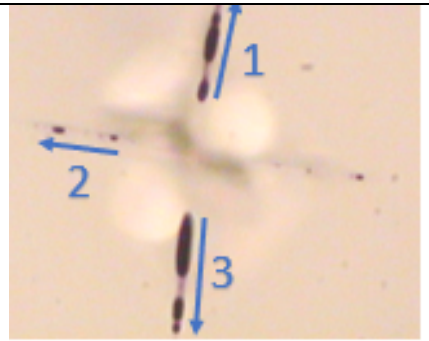 1 2 3	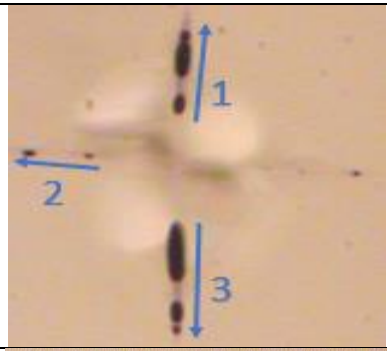 1 2 3
	10	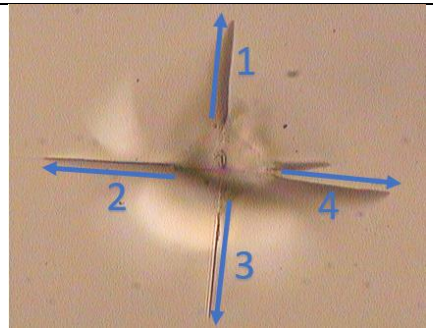 1 2 4 3	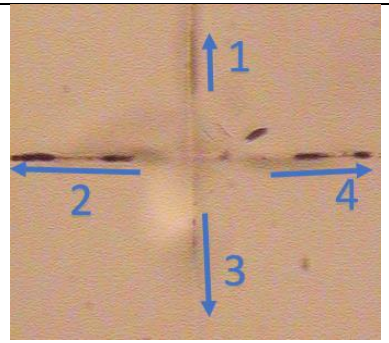 1 2 4 3	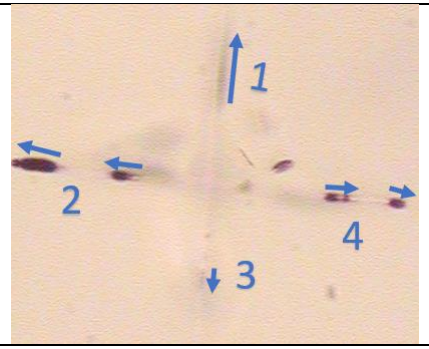 1 2 4 3	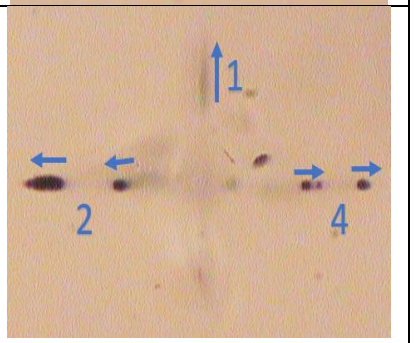 1 2 4

Table 5. Summary of quantitative experimental results for the study of annealing temperature and thermal treatment temperature effects on thermal healing abilities

Sample 1: Annealed at T=570°C and Thermal Treated at T=600°C

Conditions	Length (microns)											
	Before Thermal Treatment				After 12 Hours				After 24 Hours			
Crack No.	1	2	3	4	1	2	3	4	1	2	3	4
1	59.3	64.6	63.3	57.0	51.0	60.1	53.0	57.6	50.1	60.0	51.2	56.6
2	48.4		50.1	53.9	47.6		46.7	49.4	41.6		47.1	49.8
3	46.9	51.9	49.2	59.9	43.6	46.1	48.1	52.1	43.2	46.7	41.7	49.0
4	49.6	55.5	48.9	55.1	49.0	49.9	46.5	49.2	43.2	48.3	43.4	50.4

Conditions	Length (microns)							
	After 36 Hours				After 48 Hours			
Crack No.	1	2	3	4	1	2	3	4
1	48.1	57.3	50.1	54.5	44.9	55.8	48.7	53.1
2	41.6		45.2	47.5	41.4		40.2	45.7
3	39.9	42.9	41.4	45.9	36.6	44.0	40.1	44.9
4	40.5	46.5	39.9	47.8	37.6	43.2	41.5	49.0

Sample 2: Annealed at T=550°C and Thermal Treated at T=600°C

Conditions	Length (microns)											
	Before Thermal Treatment				After 12 Hours				After 24 Hours			
Crack No.	1	2	3	4	1	2	3	4	1	2	3	4
1	53.6	48.9	51.9	63.5	52.0	46.3	50.1	51.2	53.4	52.8	50.2	55.6
2	49.0	55.4	54.4	50.6	45.2	51.6	48.3	50.3	48.2	53.5	48.5	49.2
3	47.9	58.1	52.1	49.6	49.4	56.1	46.3	63.4	52.2	61.9	51.7	60.4
4	53.7	56.1	50.4	59.3	44.2	58.5	45.5	48.8	47.1	53.1	48.7	51.4

Conditions	Length (microns)							
	After 36 Hours				After 48 Hours			
Crack No.	1	2	3	4	1	2	3	4
1	53.4	54.0	47.8	55.2	50.7	54.3	48.5	55.4
2	46.9	54.1	49.5	50.9	49.5	53.6	50.3	51.9
3	51.2	58.7	60.7	49.7	52.2	58.0	51.6	61.5
4	44.6	50.8	47.2	51.9	44.5	51.8	52.1	51.9

Sample 3: Annealed at T=550°C and Thermal Treated at T=570°C

Conditions	Length (microns)											
	Before Thermal Treatment				After 12 Hours				After 24 Hours			
Crack No.	1	2	3	4	1	2	3	4	1	2	3	4
1	46.3	52.5	50.4	47.2	41.5	50.4	44.5	44.1	37.6	44.3	45.1	45.7
2	51.3	56.3	51.3	57.8	45.1	48.5	42.0	49.9	44.8	48.1	46.6	44.4
3	53.2	57.8	54.9	56.8	49.7	52.2	44.8	45.9	48.6	49.3	47.1	46.5
4												

Conditions	Length (microns)							
	After 36 Hours				After 48 Hours			
Crack No.	1	2	3	4	1	2	3	4
1	35.7	46.3	36.2	41.2	36.5	31.0	42.4	39.1
2	43.8	44.6	43.5	49.0	43.8	44.6	43.5	48.4
3	41.7	50.0	42.4	44.4	44.1	47.6	43.7	39.9
4								

Table 6. Summary of quantitative experimental results for the study of water pre-treatment and thermal healing abilities

Sample 1: No Water Pre-Treatment

Condi-tions	Length (microns)															
	Before Thermal Treatment				After 8 Hours				After 18 Hours				After 35 Hours			
Crack No.	1	2	3	4	1	2	3	4	1	2	3	4	1	2	3	4
1	156.9	169.2	176.6	186.0	164.1	173.7	164.1	191.5	161.9	164.9	156.9	189.9	159.1	165.6	152.6	187.4
2	161.8	159.0	158.7	177.0	157.5	192.1	163.9	189.1	156.4	188.5	160.5	181.9	140.2	181.1	151.6	172.7
3	160.3	186.6	181.6	173.8	158.2	193.1	161.8	193.1	161.2	183.8	157.8	187.6	154.7	172.4	141.1	181.6
4	155.6	189.3	158.1	183.3	158.4	191.2	166.0	184.0	154.6	190.9	163.4	178.2	145.0	178.8	157.7	176.6
5	158.3	165.1	167.0	184.5	163.8	172.9	166.2	177.6	131.5	167.6	161.0	179.5	130.2	170.5	152.9	172.0
6	169.3	189.2	171.8	168.2	147.1	187.1	172.4	183.0	146.8	178.7	165.7	171.0	146.3	175.6	160.6	167.4
7	137.9	189.5	168.0	185.6	109.9	182.3	159.5	161.2	107.9	181.2	154.2	153.6	99.6	169.7	152.6	144.6
8	162.0	170.4	173.2	192.4	168.9	177.3	165.1	200.2	162.6	174.2	165.7	193.0	161.4	162.6	164.6	185.7
9	158.5	186.3	170.2	194.2	167.3	182.6	166.5	185.8	149.5	174.4	168.3	187.0	149.2	167.0	161.0	177.4
10	153.9	176.2	180.3	191.8	154.0	179.3	156.1	178.3	154.7	142.9	156.0	189.0	143.7	131.9	146.5	180.6

Sample 2: Pre-Treated with 55% Relative Humidity

Condi-tions	Length (microns)															
	Before Thermal Treatment				After 17 Hours				After 27 Hours				After 35 Hours			
Crack No.	1	2	3	4	1	2	3	4	1	2	3	4	1	2	3	4
1	141.2	153.1	146.1	163.0	100.7	20.1	163.0	127.0	88.1	19.0	154.7	58.1	0.0	144.2	35.2	151.1
2	139.2	168.1	139.0	148.0	129.1	99.1	99.0	70.1	131.2	0.0	65.3	45.4	151.0	138.1	70.0	43.0
3	128.2	152.3	134.2	132.0	143.0	25.0	127.2	137.1	139.4	0.0	122.6	52.6	144.0	0.0	104.2	24.0
4	117.4	131.2	118.0	149.0	162.0	11.2	154.2	41.2	140.7	41.0	147.3	22.8	0.0	49.2	0.0	151.0
5	132.1	161.8	150.0	133.7	144.1	44.0	108.1	69.0	131.0	150.3	0.0	19.2	137.1	0.0	63.0	47.0
6	111.9	133.4	154.1	159.3	110.0	121.2	130.0	17.1	98.7	114.2	74.8	17.0	143.0	0.0	66.0	23.2
7	128.0	156.2	154.1	121.4	0.0	151.6	144.1	135.2	0.0	128.3	111.6	130.0	0.0	139.2	67.3	81.5

8	130.0	174.1	154.6	183.2	146.0	0.0	112.0	110.1	112.6	0.0	155.6	84.3	128.0	0.0	153.1	94.1
9	162.5	184.0	160.4	185.5	48.0	31.1	168.0	36.0	146.7	86.8	159.9	5.0	132.4	73.2	181.0	0.0
10	135.5	174.2	147.0	161.9	69.0	148.0	38.0	110.0	80.2	75.5	13.0	39.1	56.0	99.0	0.0	38.1

Experiment #1: Examine the effects of annealing conditions and glass transition temperatures on the self-healing ability of SLS glass

After annealing pre-treatment was implemented, the Vickers indentation introduced onto the three 4-mm SLS glass samples with varying annealing conditions did not have any distinguishable characteristics. All of the radial cracks' lengths fall within the range between 46.3 microns and 64.6 microns.

The radial cracks for all samples decreased in length post thermal healing process, implying the effectiveness of heat treatment. However, the degree of healing differs for each condition. The combination of annealing and thermal treatment conditions that yielded the most remarkable healing ability takes place in Sample 3, which was annealed at 550^{o}C and thermally treated at 500^{o}C, resulting in 10.9 microns average decrease in crack length for all Vickers indentation. In contrast, Sample 2 that was annealed at 550°C and thermally treated at 600°C had the least outstanding performance with only 1.0 microns average decrease in crack length, which was 90.5 percent worse in comparison to Sample 3. A 9.8-micron crack length decrease occurred for Sample 2, which was annealed at 570°C and thermally treated at 600°C. Compared to the healing capability of Sample 3, the thermal treatment in Sample 2 resulted in a 10.2 percent less effective.

Even though there was an overall reduction in crack lengths for the samples, the radial cracks were not continuously decreasing in size. In fact, crack propagation occurred dominantly within the first 18 hours of thermal treatment with an average increase of 0.6 microns, 3.6 microns, and 1.9 microns in length for Sample 1, 2, and 3 respectively. Sample 2 specifically experienced higher crack propagation than the other two samples, which then led to the overall small crack length decrease post-thermal treatment process. This could draw a relationship between the

annealing and thermal treatment conditions and the crack propagation effects and how they all tie up with the healing efficiency.

Another noteworthy observation that can be made is the increase in width with time as thermal healing was conducted. This was evidenced by the darker regions at the radial cracks in the later stages of the process compared to the beginning phases, as demonstrated in the microscope-captured images of the Vickers indentation in Appendix B. Qualitative results indicate a larger width increase took place in Sample 1 where higher annealing temperature (570°C) and thermal treatment temperature (600°C) were implemented. Sample 2 showed some increase in width over time although it was not as significant as Sample 1. In comparison, Sample 3 had the smallest width change throughout the thermal treatment time. A possible correlation between the width increase and thermal healing temperatures could be made, yet further measurement on the radial crack's width is required. This subject is not within the scope of this thesis.

Experiment #2: Evaluate the pre-treatment effects with water of SLS glass on its self-healing properties

Vickers indentation was introduced onto the two 1-mm glass samples after appropriate pre-treatment conditions were carried out. The radial cracks in Vickers indentation between the two samples did not vary significantly. All the crack lengths fall within the range between 111.8 microns and 186.0 microns.

While there was an overall decrease in the radial crack lengths for both samples with and without water pre-treatment after thermal healing was carried out, the sample that was pre-treated with 55% RH performed significantly better in terms of self-healing ability. More specifically, the average decrease in crack length for Sample 1 without water pre-treatment was 12.6 microns,

whereas the decrease for Sample 2 with 55% RH pre-treatment was 74.5 microns. This means that water pre-treatment increased the self-healing capability of SLS glass by approximately 6 times.

Similar to the observations made in *Experiment 1*, crack propagation also took place in the first 8 hours of the thermal healing process for both samples, although Sample 2 experienced significantly higher crack propagation than Sample 3. The average length increase due to crack propagation for Sample 2 is 7.7 microns and for Sample 3 is 18.6 microns. The presence of water from the pre-treatment conditions could lead to a higher crack propagation in thermal treatment.

Crack healing takes place via a "pinch off" mechanism. Instead of having uniform length reduction from the tip of the radial cracks, glass heals differently in various regions, thus resulting in discontinuity in cracks. This phenomenon was found dominantly for Sample 2, particularly in Crack 1, 3, 4, 9, and 10 shown in Appendix B, where unsteady healing leads to oval cavities pinched off from cracks, leaving some fragments of the cracks opened. Compared to other glass samples with different pre-treatment and thermal treatment conditions, this sample exhibited higher healing ability and almost reached completion as indicated by the absence of the majority of the crack. Hence, this implies that the "pinch off" mechanism only occurs towards the end of the healing cycle and not at the beginning of the process.

The same phenomenon of increasing crack width over time is also observed in *Experiment 2*, as demonstrated by the darker regions in the radial cracks in the latter phases of the thermal healing process. Direct observations of microscope-captured images show that the width increase happens at a much earlier stage for Sample 2 comparing to Sample 1, implying the effects of water pre-treatment on the crack width evolutions. Further measurements are required to deduce the relationship between the crack width increase and the pre-treatment effects. This is not within the scope for this thesis.

Discussions

Thermal healing mechanism governed by viscous flow and capillary forces

Glass healing capability could be explained via two proposed mechanisms that govern the necessary morphological alterations – viscous flow and capillary forces.

Simply defined, viscous flow is a type of fluid flow where continuous steady motion of particles takes place as a respond to fluid inertia and/or pressure gradients (Kundu, 2012). Thermal healing is proposed to be closely associated with Nichols and Mullins' theory of local surface perturbation, where a surface of revolution evolves due to mass transport mechanism governed by viscous flow (Cassidy, 1970 and Nichols, 1965). It has been observed that crack closure is a result of viscous relaxation of glass in the region crack tip (Girard, 2011). Similar to the local heating phenomenon of indentation under the diamond, anomalous viscous flow accounted for by sufficient viscosity drives critical morphological changes (Marsh, 1964).

Capillary force refers to forces that seek to reduce the surface and shape the material volume to a point where lowest surface tension forces potential is favored. Many literature papers offer an explanation to thermal healing by examining its correlation with capillary forces. Girard et. al. proposed that changes in radial crack morphology are guided by capillary forces, where the reduction of total surface energy of the system can be obtained by direct reduction of crack surfaces through smoothing, rounding, and flattening. Since capillary force is a function of relative humidity and temperature, thermal treatment conditions provide sufficient driving forces that allow for crack closure (Chen, 2008).

Thermal treatment temperature and annealing temperature effects on thermal healing

The glass samples were treated at different thermal treatment temperatures to evaluate its effects on thermal healing. The experimental samples were healed at different temperatures (600°C and 500°C). The results showed that the sample treated 500°C carried out better thermal healing performance than that at 600°C. This could be explained by the inverse proportional relationship between viscosity and temperature based on Fulcher equation,

$$log_{10}\eta = A + \frac{B}{T - T_o}$$

where η is viscosity, T is temperature, and A, B, and T_o are constants derived experimentally (Fulcher, 1925). Higher thermal treatment temperature leads to lower viscosity assisting viscous flow, thus heals faster.

To examine the effects of annealing temperatures on thermal healing, different annealing temperatures were carried out for the glass samples (550°C and 570°C). From the experimental results, the sample annealed at 570°C performed much better in healing capability compared to that at 550°C. This could be due to the insufficient annealing that fails to relieve all residual stress, hence affects the overall uniformity of the glass surface. As a result, the lower annealed temperature glass did not perform healing as well as the higher annealed temperature sample. However, future experiments are needed to further explore this concept.

Water pre-treatment effects on thermal healing

The water pre-treatment effects on thermal healing were studied by performing different pre-treatment procedures on glass samples. It showed that the pre-treatment process played a crucial role in enhancing the thermal healing capability in glass. This indicates that water dissolved around cracks during pre-treatment in high water vapor environment and the increased water

content in glass surface reduced viscosity during thermal treatment, facilitating the crack healing process. The increasing water content in glass is observed to reduce viscosity by orders of magnitude around the glass transition temperature (Gaudio, 2007). The observed faster rate of crack smoothing is consequently consistent with a lowering of viscosity based on the proposed principle of viscous flow in thermal healing (Girard, 2011).

Crack propagation and pinch-off healing model

The thermal healing process was proposed by Hrma et. al. to follow a four-stage morphological changes:

(i) *Relaxation and blunting*: Residual stresses introduced by Vickers indentation are allowed to relax due to capillarity-driven viscous flow of glass.

(ii) *Receding and breaking up*: The crack area decreases due to the inward motion of crack boundaries while impression zones are progressively filled by inflowing glass and oval cavities are pinched off from radial cracks.

(iii) *Rounding and grooving:* Grooving takes place for crack edges while oval cavities rounding occurs for subsurface cracks.

(iv) *Smoothing and spheriodizing:* Confined gas entrapment helps smoothen the glass surface.

Crack propagation falls within the *relaxation and blunting* phase due to its sole activity within the first 18 hours of treatment. Subsequently, the pinch-off healing process takes place in the *receding and breaking up* phase, where the healing model is frequently referred to as “peninsulas and islands of healed areas grew until the crack broke up into separated lakes.” The

subsurface glass healing mechanism in thermal treatment included pinch-off into voids which appeared quasi-circular in cross-section as crack closure happened gradually (Wilson, 1997).

Chapter 4

Conclusions and Further Work

Summary of Findings

To comprehend the self-healing mechanism of soda-lime silicate glass in thermal treatment and the different factors that drive its efficiency, the experiment examined the effects of thermal healing temperatures, annealing conditions, and water pre-treatment on glass healing capability. The proposed healing mechanism is based off of morphological changes on glass subsurface that could be governed by viscous flow and capillary forces. It was observed that the glass sample thermally treated at a lower thermal treatment temperature performed better in healing, possibly due to the lower viscosity associated with higher temperature as described by Fulcher equation. Moreover, higher annealed temperature glass also carried out better healing performance than lower annealed temperature glass; however, insufficient annealing could have taken place that resulted in failure to relieve residual stress, thus future experiments are needed to further explore this concept. Thermal healing was significantly improved with water pre-treatment due to the viscosity effects and water-glass interactions. Crack propagation and pinch-off healing model were two phenomena that took place as part of thermal treatment process in soda-lime silicate glass.

Suggestions for Further Work

The following suggestions could be promising directions for future work on the study of self-healing mechanisms of glass:

1. **Further execution on the study of annealing conditions and glass transition temperatures effects on self-healing capability of soda-lime silicate glass:** While this experiment provides preliminary data to offer a general comprehension on the effects of annealing and glass transition temperature on thermal healing, more experimental data should be collected for a more comprehensive understanding.
2. **Execute tribological tests on thermally-healed soda-lime silicate glass:** After radial cracks are completely healed from thermal treatment (i.e. radial cracks are no longer visibly traced on the glass surface), tribological tests should be carried out in regions where Vickers indentation were introduced to understand the glass wear behaviors after thermal healing and to examine if the crack re-opens (i.e. if healing is only performed at subregion of the glass surface).
3. **Execute three-point bending tests on thermally-healed soda-lime silicate glass:** Thermal treatment is crucial in implementing self-healing in soda-lime glass, but further experiment execution must be carried out to study the strengthening effects of glass after the healing process as the interference of water vapor could potentially decrease the Young Modulus of the as-received glass.

BIBLIOGRAPHY

Achintha, M. “Chapter 5: Sustainability of Glass in Construction.” *Sustainability of Construction Materials (Second Edition).* Woodhead Publishing Series in Civil and Structural Engineering, 2016.

Ashby, Michael. “Chapter 15: Material Profiles.” *Materials and the Environment (Second Edition).* Netherlands: Elsevier, 2013.

ASTM E384, “Standard Test Method for Knoop and Vickers Hardness of Materials.” ASTM International, West Conshohocken, PA, 2017.

Benvenuto, Mark Anthony. “Industrial Chemistry: For Advanced Students.” Berlin: Walter de Gruyter GmbH & Co KG., 2015.

Berger, Michael. “Smart Glass Coatings for Energy-Efficient Eco-Homes.” Nanowerk, 2 February 2012.

Burghard, Zaklina, Andre Zimmerman, Jurgen Rodel, Fritz Aldinger, and Brian R. Lawn. “Crack Opening Profiles of Indentation Cracks in Normal and Anomalous Glasses.” *Acta Materialia,* 52 (2): 293-297, 2004.

Cassidy, D.C. and N.A.Gjostein. “Capillarity-Induced Smoothing of Glass Surface by Viscous Flow.” *Journal of American Ceramic Society,* 53 (3): 161-168, 1970.

Change, Tian-Ci, Xun Cao, Shan-Hu Bao, Shi-Dong Ji, Hong-Jie Luo, and Ping Jin. “Review on Thermochromic Vanadium Dioxide Based Smart Coatings: From Lab to Commercial Application.” *Advances in Manufacturing,* 6 (1): 1-19, 2018.

Chen, S.H. and A.K. Soh. “The Capillary Force in Micro- and Nano-Indentation with Different Indenter Shapes.” *International Journal of Solids and Structures,* 45 (10): 3122-3137, 2008.

Chorfa, Abdellah, Hamidouche Mohamed, Abderrahim Madjoubi, and Fabrice Petit. “Mechanical Behaviors of Glass During Cyclic Instrumented Indentation.” *Materials Science – Poland,* 28 (1), 2010.

Estes, Adam Clark. “The Pyrex Glass Controversy That Just Won’t Die.” *Gizmodo,* 2019.

Fulcher, G. S. “Analysis of Recent Measurements of Viscosity of Glass.” *Journal of American Ceramic Society,* 8 (6), 339, 1925.

Gaudio, P. Del, H. Behrens, and J. Deubener. “Viscosity and Glass Transition Temperature on Hydrous Float Glass.” *Journal of Non-Crystalline Solids,* 353, 223-6, 2007.

Girard, Remi, Annelise Faivre, and Florence Despetis. “Influence of Water on Crack Self-Healing in Soda-Lime Silicate Glass.” *Journal of American Ceramic Society,* 94 (8): 2402-2407, 2011.

Haldimann, Matthias, Andreas Kuible, and Mauro Overend. “Chapter 1: Material.” *Structural Use of Glass.* Zurich: International Association for Bridge and Structural Engineering, 2008.

Hasanuzzaman, Muhammad, Aran Rafferty, Mustafa Sajjia, and Abdul Ghani Olabi. “Properties of Glass Chemicals.” 2016. DOI 10.1016/B978-0-12-803581-8.03998-9.

Hrma P., W. T. Han, and A. R. Cooper. “Thermal Healing of Cracks in Glass.” *Journal of Non-Crystalline Solids,* 102: 88-94, 1988.

Karazi, S. M., I. U. Ahad, and K. Y. Benyounis. "Laser Micromachining for Transparent Materials." *Materials Science and Materials Engineering,* 2017. DOI 10.1016/B978-0-12-803581-8.04149-7.

Mancuso, Elena, Oana A. Bretcanu, Martyn Marshall, Mark Birch, Andrew McCaskie, and Kenneth Dalgarno. "Novel Bioglasses for Bone Tissue Repair and Regeneration: Effect of Glass Design on Sintering Ability, Ion Release, and Biocompatibility." *Material Design,* 129: 239-248, 2017.

Marsh, D. M. "Plastic Flow in Glass." *Royal Society,* 279, 1378, 1964.

Mathers, Gene. "Hardness Testing Part 1." TWI Global. https://www.twi-global.com/technical-knowledge/job-knowledge/hardness-testing-part-1-074.

Mauro, John. "Lecture 10 – Silicate and Aluminosilicate Glasses." The Pennsylvania State University, University Park. October 2019. PowerPoint presentation.

Mauro, John. "Lecture 17 – Hardness of Glass." The Pennsylvania State University, University Park. October 2019. PowerPoint presentation.

McMillan, Peter Warwick. "Glass Ceramics." London: Academic Process, 1979.

Nichols, F.A. "Morphological Changes of a Surface of Revolution Due to Capillary-Induced Surface Diffusion." *Journal of Applied Physics,* 36: 1862, 1965.

Paul, A. "Chemistry of Glasses, 2nd edition." New York: Chapman and Hall, 1990.

Sanders, Thomas H. "Viscosity Behavior of Oxide Glass." *Coursera.* https://www.coursera.org/lecture/material-behavior/6-5-viscosity-behavior-of-oxide-glasses-IIkka.

Sagadevan, Suresh and Edison Chandraseelan. "Applications of Chalcogenide Glasses: An Overview." *International Journal of ChemTech Research,* 6 (11): 4682-2686, 2014.

Sempolinski, Daniel R. and Paul M. Schermerhorn. “Silica, Vitreous Silica.” *Kirk-Othmer Encyclopedia of Chemical Technology.* New Jersey: John Wiley & Sons, 2000.

Seward III, Thomas B. and Terese Vascott. “High Temperature Glass Melt Property Database for Process Modelling.” *The American Ceramic Society.* Ohio: Westerville, 2005.

Smith, R. L. and G. E. Sandland. “An Accurate Method of Determining the Hardness of Metals, with Particular Reference to Those of a High Degree of Hardness.” *Proceedings of the Institution of Mechanical Engineers,* Vol. I, 623-641, 1922.

Schneider, C. A., W. S. Rasband, and K. W. Eliceiri. “NIH Image to ImageJ: 25 Years of Image Analysis.” *Nat Methods,* 9 (7): 671-675, 2012.

“The Glass Age – Science of Glass.” Corning. https://www.corning.com/worldwide/en/innovation/the-glass-age/science-of-glass.html.

Varshneya, Arun K. and John C. Mauro. “Fundamentals of Inorganic Glasses, 3rd edition.” Netherlands: Elsevier, 2019.

Vogel, Werner. “Glass Chemistry.” Springer-Verlag Berlin and Heidelberg GmbH & Co. K; 2nd revised edition. 1994.

Wananuruksawong, R., S. Jinawath, P. Padipatvuthikul, and T. Wasanapiarnpong. “Fabrication of Silicon Nitride Dental Core Ceramics with Borosilicate Veneering Material.” *IOP Conference Series: Materials Science and Engineering,* Volume 18, Symposium 13, 2011.

Wilson, B.A. and E.D. Case. “In Situ Microscope of Crack Healing in Borosilicate Glass.” *Journal of Materials Science,* 32 (12), 3163-3175, 1997.

ACADEMIC VITA

TRAN HA-QUYNH NGO (TRISCA)
trisca_ngo@yahoo.com

EDUCATION

The Pennsylvania State University – Schreyer Honors College December 2019 (Graduate)
Bachelors of Science in Chemical Engineering
Mathematics Minor

INDUSTRY EXPERIENCE

Procter & Gamble, Binh Duong Plant, Vietnam June 2019- August 2019
Process Engineering Intern

- Identified the root causes for a recurring manufacturing problem faced by multiple plants in Asia in the Fabric & Home Care division
- Implemented optimized solutions to foster $54K in net savings by reducing effort and productivity loss
- Enhanced process efficiency by 4% by reducing time loss caused by the gap between the quality assurance and operation process

King Nutronics Corporation, Woodland Hills, California January 2019 - May 2019
Research & Engineering Co-Op

- Designed from scratch an automated instrument cleaning system for pressure gauges to accommodate U.S. Navy and NASA operations, generating $8M in company net revenues
- Improved the shelf-life of thermo units by replacing the current insulating system with a more compatible material, increasing the product market value by 30%
- Took initiatives in executing on-site passivation process for stainless steel part (ASTM A967), reducing production costs by 3%
- Executed quality assurance on electric printed circuit boards (PCBs) and documented transducer readings

RESEARCH EXPERIENCE

Glass Surface Science Research Project, Penn State University August 2016 - December 2019
Materials Science Research Assistant

- Examined the self-healing properties of soda-lime silicate glass under specialized thermal conditions
- Investigated the intrinsic mechanical responses and the sensitivity of friction on the glass surface under different chemical reactions
- Enhanced technical skills in operating Atomic Force Microscopy (AFM), Linear Wear Testing (LWT), Three-point Bending Flexural Test

CSL Behring Fermentation Facility, University Park, Pennsylvania January 2019 - February 2019
Industrial Biotechnology Research Assistant

- Devised innovative biotherapies for treating serious and chronic medical conditions, specifically different cancer types
- Executed fermentation runs to produce gram-quantity of recombinant proteins

- Achieved excellence in operating upstream and downstream research and process development services

Soltis Center & Campanario Biological Site, Costa Rica December 2018 - August 2019
Biological Research Assistant

- Conducted 2 faculty-led research projects and 1 independent research project that were field-intensive with a heavy focus on ecology, evolution, behavior and population biology of local plants and animals
- Composed formal write-ups for each research project and presented orally to Penn State and Costa Rican faculty members
- Applied biostatistics to analyze complex data and carry out graphical representations

Layered Inorganic Materials Research Project, Penn State University August 2017 - May 2018
Chemistry Research Assistant

- Evaluated laboratory procedures on topochemically interconverting structural families of layered and three-dimensionally bonded oxides
- Acquired technical skills in X-Ray Photoelectron Spectroscopy (XPS) and Ultraviolet (UV)

TEACHING EXPERIENCE

Physics 211 (General Physics: Mechanics), Penn State University August 2016 - December 2016
Teaching Assistant

- Assisted professors in lectures to provide an interactive learning environment for over 130 students
- Conducted weekly one-hour tutorial sessions and exam reviews to reinforce important physics concepts, review materials, and help with homework
- Led small group discussions to uncover misconceptions and develop deeper understanding of course materials

Real Colegio Nuestra Señora de Loreto, Madrid Spain January 2017 – July 2017
Second-Grade English Teacher

- Supervised 43 elementary students and communicated with parents about students' progress
- Created an agenda for every lecture and incorporated interactive activities to promote an English-speaking environment
- Revised and updated the teaching curriculum for the English department
- Collaborated with other English teachers in the department to prepare teaching materials

LEADERSHIP EXPERIENCE

PNC Leadership Development Center, Penn State University October 2018
Selected Honors Consultant

- 12 Schreyer Honors Scholars were selected based on a rigorous application process to participate in the prestigious program with a focus on comprehensive leadership skills development
- Analyzed interactive exercises that are modeled after programs used by companies and other organizations to identify top talents in their workforce
- Conducted team discussions to solve real-world business problems faced by leaders of various industries

Schreyer Career Development Mentoring Program, Penn State University August 2017 – May 2018

Honors Mentor

- Facilitated bonding activities within the "buddy system" in which an upperclassman is paired up with an underclassman within Schreyer Honors College
- Guided 3 underclassmen in resume reviews, course scheduling, research experience, and different career opportunities available on-campus
- Assisted newcomers with a smoother transition from high school to college

PSU Music Service Club, Penn State University August 2015 – December 2016

Secretary & Historian

- Constructed an outline for each volunteering event including the contact information of the nursing homes and elementary schools to be performed at, contact information of all the participants, the order of performances of the event, etc.
- Composed weekly emails regarding meeting reminders, upcoming events, and member-of-the-month
- Recorded each member's activities including meeting attendance, active participation at volunteering events, dues payment, etc.
- Created monthly reports to submit to the Organization Adviser and Penn State Librarian

Hospitality in Learning & Leading (HiLL) Camp, Ho Chi Minh, Vietnam May 2015 – July 2017

Camp Mentor

- Instructed ten campers in creating a hospitality-related business plan and a pitch deck to be presented in front of a panel of Cornell University panelists
- Presented the current hospitality trends and the potentials as well as drawbacks of the industry in Vietnam
- Supervised campers during hotel tours and networking events

The GLOBE Special Honors Living Option, Penn State University August 2015 – December 2016

Selected Resident

- Host and participate in group discussions, guest professor events, and food events with the aim to foster cultural and international perspectives
- Convert ideas that stimulate global awareness into beneficial actions

Vinteambuilding Summer Camp, Ho Chi Minh City, Vietnam December 2012– July 2019

Camp Founder, Organizer, and Counselor

- Worked with five other co-organizers in the timeframe of six months to bring the camp to reality
- Presented the camp scheme in front of sponsors for financial assistance
- Created an agenda for the three-day camp including different bonding and training activities that enhance leadership and teamwork skills
- Supervised 223 sixth-graders to eighth-graders

GLOBAL EXPERIENCE

Engineering-Intensive Semester Abroad in Madrid, Spain Spring 2017

- An intensive six-month studying abroad with a focus on engineering, materials science, and architecture

Entrepreneurial Leadership in Tel Aviv & Jerusalem, Israel March 2018

- Explored the innovative mindsets and pervasive entrepreneurial culture of Israel with a focus on developing leadership skills
- Networked with start-up leaders in agricultural, IT/media, high tech, and tourism industries

AWARDS AND HONORS

2nd place in Kohl's Business Case Competition with Integrity 2018
Alton R. Klinestiver Memorial Scholarship
Schreyer Academic Excellence Scholarship
Schreyer Ambassador Travel Grants
The National Society of Collegiate Scholars
Dean's List

TECHNICAL SKILLS

Microsoft Office, Microsoft Visual Studio – C++, MATLAB, Wolfram Mathematica, R Studio, Aspen+, JMP Statistical, AutoCAD, SolidWorks